Journal of Financial Economics 149 (2023) 27–51

Contents lists available at ScienceDirect

Journal of Financial Economics

journal homepage: www.elsevier.com/locate/jfec

Micro uncertainty and asset prices☆

Bernard Herskovic[a,b,*], Thilo Kind[c], Howard Kung[d,e]

[a] University of California, Los Angeles (UCLA) Anderson School of Management, United States
[b] National Bureau of Economic Research (NBER), United States
[c] Leibniz Institute for Financial Research, Germany
[d] London Business School, United Kingdom
[e] Centre for Economic Policy Research (CEPR), United Kingdom

ARTICLE INFO

Article history:
Received 27 December 2022
Revised 6 April 2023
Accepted 6 April 2023
Available online 30 April 2023

Keywords:
Production-based asset pricing
Neoclassical Investment
Long-run risks
Cross-section of returns
Micro uncertainty
TFP

ABSTRACT

Size and value premia comove strongly with one another at low frequencies, but they are both negatively related to long-run movements in the equity premium. We explain these patterns in an investment-based asset pricing model featuring persistent micro and macro uncertainty. Micro uncertainty generates size and value premia waves, while macroeconomic uncertainty produces equity premium waves. The negative correlation between micro and macro uncertainty at low frequencies explains why the equity premium is a long-term hedge for size and value premia. Persistent micro uncertainty is also a source of instability for size and value factors in short samples.

1. Introduction

Risk premia dynamics in the aggregate and cross-section of equities exhibit prolonged booms and busts. A recent example includes the equity premium surges in the bull markets of the 1990s and 2010s but a collapse in the lost decade in between. Conversely, the size and value premium performed strongly in the 2000s but slumped in the 2010s. We relate these persistent risk premia fluctuations to micro and macro uncertainty. We define micro uncertainty as the dispersion in firm total factor productivity (TFP) shocks, while macro uncertainty characterizes the standard deviation of aggregate output growth. Our paper is motivated by the following *low-frequency relations*. First, micro uncertainty exhibits strong positive comovement with size and value premia. Second, macro uncertainty comoves positively with the equity premium but negatively with micro uncertainty. Third, common variation in the size and value premia hedge against equity premium fluctuations.

We build an investment-based asset pricing model with heterogeneous firms to explain the long-run patterns linking risk premia to micro and macro uncertainty. Firms use capital as the only input to produce output with decreasing returns to scale technology, subject to aggregate and firm-specific productivity shocks. The firm-specific

☆ G. William Schwert was the editor for this article. We thank G. William Schwert (managing editor), Dimitris Papanikolaou (co-Editor), and the anonymous referee. We also thank Hengjie Ai, Ravi Bansal, Federico Belo, Gian Luca Clementi, Joao Cocco, Max Croce, Nicolas Crouzet, Vadim Elenev, Joao Gomes, Francisco Gomes, Lars Kuehn, Xiaoji Lin, Lars Lochstoer, Tatyana Marchuk, Tyler Muir, David Schreindorfer, and Lu Zhang, and participants at the London School of Economics, Goethe University, INSEAD, London Business School, Bocconi, Hong Kong University, University of Kent, Birkbeck College, Stanford Institute of Theoretical Economics Workshop, Barcelona GSE Summer Forum, SFS Cavalcade, Duke/UNC workshop, HEC-Paris Spring Conference, BI-SHoF Asset Pricing Conference, HEC-Paris Spring Conference, UBC Summer Conference, Frontiers in Macrofinance Conference for helpful comments. We thank Raksha Jangada for excellent research assistance. Bernard Herskovic is grateful to the Fink Center for Finance and Investments at UCLA Anderson for generous grant. This paper previously circulated with the title "Size Premium Waves."

* Corresponding author.
E-mail addresses: bernard.herskovic@anderson.ucla.edu (B. Herskovic), kind@safe-frankfurt.de (T. Kind), hkung@london.edu (H. Kung).

https://doi.org/10.1016/j.jfineco.2023.04.006
0304-405X/

shocks are mean reverting and feature a common stochastic volatility process that generates time-varying dispersion in observed TFP across firms (*micro uncertainty*). The aggregate productivity component is exposed to long-run consumption risks (e.g., Croce, 2014; Favilukis and Lin, 2013). There is a representative agent with Epstein and Zin (1989) recursive utility with a preference for an early resolution of uncertainty. As in Bansal and Yaron (2004), the consumption growth process includes transitory shocks and a persistent shock to the conditional mean subject to stochastic volatility (*macro uncertainty*). The negative long-run relation between micro and macro uncertainty is captured by a persistent common factor that affects micro and macro uncertainty processes in the opposite direction.

When calibrating our model to match the low-frequency dynamics of micro and macro uncertainty, we can explain the average size, value, and equity risk premia along with their comovement. A sizable equity premium arises as aggregate dividends inherit long-run risks from productivity through the balanced growth restrictions. Value (small) firms are endogenously more exposed to long-run risks than growth (big) firms, leading to a value (size) premium. The conditional dynamics of the cross-sectional and aggregate risk premia are due to variations in micro and macro uncertainty. Fluctuating micro uncertainty generates time-varying dispersion in conditional betas on aggregate consumption risks (e.g., Santos and Veronesi, 2004) while fluctuating macro uncertainty produces time-varying market prices of risk. Our model calibration implies that persistent micro uncertainty dominates the common long-run variation of size and value premia. In contrast, persistent macro uncertainty governs the dynamics of the equity premium. The negative link between persistent components of micro and macro uncertainty implies that the equity premium negatively correlates with the size and value premia at low frequencies. We also show that persistent micro uncertainty is a source of instability for value and size factors in short samples.

The firm TFP shock structure and investment frictions featured in the model are critical for generating sizable unconditional size and value premia. Measured firm TFP consists of a mean-reverting firm-specific component that multiplies the aggregate trend component that depends on long-run consumption risks. The firm-specific component, therefore, affects firm exposure to long-run risks. Firms can shed exposure to aggregate risks through capital accumulation decisions, but with limits due to investment frictions. These frictions include fixed costs that are non-proportional and proportional to the capital stock and asymmetric capital adjustment costs (e.g., Zhang, 2005).

Mean-reverting firm-specific productivity shocks help to produce a size effect in our model (e.g., Babenko et al., 2016; Clementi and Palazzo, 2019). Small market cap firms have small capital stock and low productivity today. Due to mean reversion, the future growth rate of productivity is expected to be high, exposing the cash flows of small firms more to long-run risks. Small firms also have limited capital stock that they can liquidate to hedge bad aggregate shocks and face high disinvestment costs that further reinforce their high exposure to long-run risks. Large market cap firms have large capital stock and high productivity. Mean reversion implies that the cash flows of these firms have lower exposure to long-run risks. Therefore, the cash flows of small firms have higher exposure to long-run risks than big firms, leading to a positive size premium.

Operating leverage and asymmetric adjustment costs contribute to a value premium, in line with work by Zhang (2005), Belo et al. (2014a), and Donangelo (2016). High book-to-market (value) firms are characterized by low productivity and large capital stock. The low productivity today means that the productivity growth of value firms is more exposed to long-run risks due to mean reversion. However, value firms have strong incentives to liquidate their large and unproductive capital to finance larger payouts that would hedge their higher exposure to long-run risks, but are limited by high disinvestment costs and operating leverage. Therefore, investment frictions ensure that the cash flows of value firms are highly exposed to long-run risks. Low book-to-market (growth) firms are associated with high productivity and low capital. High productivity implies growth firms are less exposed to long-run risks due to mean reversion, but they have strong incentives to invest. Capital adjustment costs prevent growth firms from investing aggressively, reinforcing their lower cash flow exposure to long-run risks.

The persistent common factor of micro and macro uncertainty drives the low-frequency dynamics of risk premia through distinct channels. We can characterize these channels using an approximate equilibrium factor structure for returns implied by our model, where exposure to long-run consumption risk is the main determinant of expected returns. The effect of the common uncertainty factor on micro uncertainty generates time-varying dispersion in cash flow exposures to long-run risks across size and book-to-market sorts. Higher micro uncertainty directly increases the magnitude of the firm-specific productivity shocks, which magnifies the dispersion in productivity growth exposures to long-run risks across characteristics. Investment frictions ensure that the dispersion of cash flow exposures and conditional betas also rises, producing larger size and value premia. Persistent micro uncertainty, therefore, contributes to strong positive comovement between size and value premia.

The effect of the persistent common uncertainty factor on macro uncertainty generates time-variation in the market price of long-run risks in our model. This channel drives the fluctuations in the equity premium in our model, while cross-sectional risk premia are affected by variations in both the market price of risk and the dispersion in conditional betas. As the common uncertainty factor impacts micro and macro uncertainty in opposite directions, the movements in the market price of risk hedge the dispersion in conditional betas. Our benchmark calibration suggests that the time-varying dispersion in conditional betas dominates opposing movements in the market price of risk for size and value premia, allowing the model to explain the strong positive correlation between size and value premia but their negative correlation with the equity premium at low frequencies.

We find strong empirical support for the link between cash flow risk exposures across characteristics and persistent micro uncertainty featured in our model. We construct cash flow risk exposures with respect to long-run risks for each size and book-to-market deciles by regressing payout growth on a measure of long-run consumption risks following Bansal et al. (2005). We first verify that the average cross-sectional relationship between the cash flow betas and expected returns is positive. Then we show that the dispersion in cash flow betas across a given characteristic increases with micro uncertainty, in line with model predictions.

We show that persistent micro uncertainty is a source of instability in size and value premia in short samples. Periods of low micro uncertainty compress the distribution of cash flow betas across characteristics, reducing size and value premia and weakening their statistical significance in short samples. This margin helps explain the empirical observation that size and value premia are insignificant when micro uncertainty is low but significant when micro uncertainty is high. Overall, our paper highlights the importance of time-varying micro uncertainty for explaining asset prices.

Our paper relates to an extensive literature studying the cross-section of stock returns in production-based models in partial equilibrium (e.g., Berk et al., 1999; Carlson et al., 2004; Zhang, 2005; Kogan and Papanikolaou, 2014; Liu et al., 2009; Gomes and Schmid, 2010; Belo and Lin, 2011; Belo et al., 2014b; Kuehn et al., 2017) and in general equilibrium (e.g., Gomes et al., 2003; Favilukis and Lin, 2013; 2015; Bai et al., 2019). We build on this literature by illustrating how incorporating a common persistent factor in micro and macro uncertainty can account for the comovement of the size, value, and equity premia at low frequencies.

Our framework relates to heterogeneous firm models examining the effects of uncertainty shocks on investment and financing choices (e.g., Bloom, 2009; Gourio and Michaux, 2012; Alfaro et al., 2018; Kuehn et al., 2016). We complement this literature by highlighting the role of micro and macro uncertainty fluctuations at low frequencies on asset price dynamics. Micro uncertainty generates size and value premia waves by generating time-varying dispersion in conditional betas, while macro uncertainty produces equity premium waves by producing a time-varying market price of risk.

We also relate to models examining the asset pricing implications of time-varying idiosyncratic cash flow risks (e.g., Santos and Veronesi, 2004; Menzly et al., 2004; Ai and Kiku, 2015; Herskovic et al., 2016; 2020; Dew-Becker and Giglio, 2020). We contribute to this literature by illustrating how the persistent common component in firm-specific uncertainty drives the low-frequency dynamics of the size and value premia, and that this common component is negatively associated with both the equity premium and aggregate uncertainty.

The paper is organized as follows. Section 2 outlines the data and key stylized facts. Section 3 describes the benchmark model. Section 4 presents the quantitative evaluation of the model. Section 5 concludes.

2. Low-frequency empirical relations

This section describes the data series and the key stylized facts. We document the following low-frequency empirical relations: (i) micro uncertainty positively correlates with size and value premia, (ii) macro uncertainty positively relates to the equity premium but negatively comoves with micro uncertainty, and (iii) size and value premia exhibit positive comovement, but both negatively correlate with the equity premium. The model presented in Section 3 is used to explain these empirical relations.

2.1. Data description

Aggregate data for consumption, output and total factor productivity (TFP) are from the Federal Reserve Economic Data (FRED). Consumption is computed as real personal consumption expenditures. Output is calculated using real gross domestic product. Aggregate total factor productivity (TFP) is computed at constant national prices according to Feenstra et al. (2015). Returns for the market, size, book-to-market portfolios, and riskfree rate are from Kenneth French's website. We define the equity premium as the difference between the market portfolio return and the riskfree rate, and we compute a 10-year forward rolling window average from year $t+1$ to year $t+10$. Similarly, we define the size (value) premium as the spread portfolio return between the smallest (highest) and the largest market cap (lowest book-to-market) deciles and compute a 10-year forward rolling window average from year $t+1$ to year $t+10$.[1]

Total payouts for the size and book-to-market portfolios are measured by computing firm *cum-* and *ex*-dividend returns adjusted for repurchases following Bansal et al. (2005). The data for constructing payouts are from the Center for Research in Security Prices (CRSP). Appendix A.1 contains the details for calculating the payouts. Firm-level capital stock, employment, and investment measures are constructed with Compustat data. The return sample is available from 1925 to 2020, while the Compustat data used is from 1963 to 2020. We compute the low-frequency components of the data series by applying the Christiano and Fitzgerald (2003) bandpass filter to isolate frequencies between 25 and 50 years.[2]

2.2. Micro uncertainty

We define micro uncertainty as the cross-sectional dispersion in firm TFP. To measure micro uncertainty, we first compute the log TFP of firm i as the residual (z_{it}) from the

[1] The stylized facts documented below are robust to alternative constructions of the size premium, such as excluding January returns or sorting based on different size measures (e.g., sales, book equity, or total sales). However, all these versions for the size premium comove strongly with one another and, in particular, with the size premium based on market capitalization. Such return comovement across different size-based strategies is depicted in Fig. A.1 in the Appendix, where we plot all these different versions for the size premium.

[2] Table A.1 in the Appendix shows the robustness of our results by varying the frequencies of the filter.

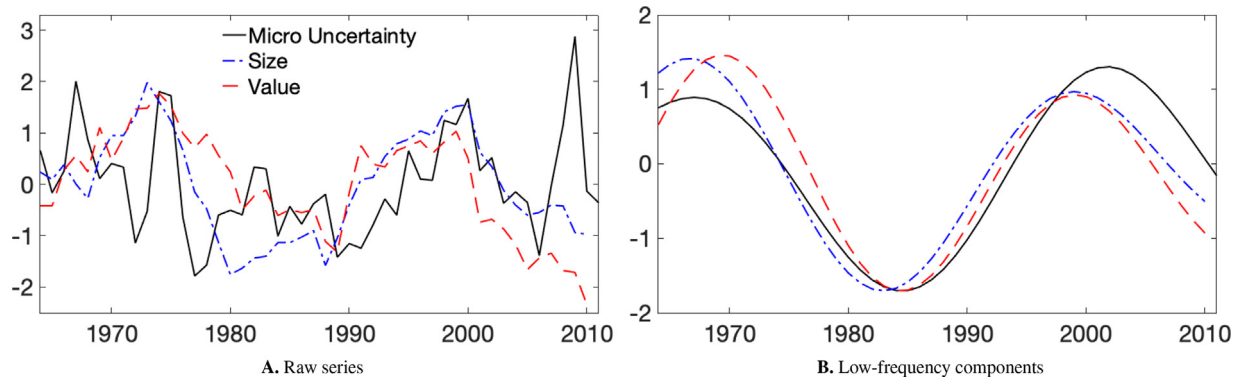

Fig. 1. Micro uncertainty, size premium, and value premium.
This figure shows the time series comovement between the following variables: small minus big decile portfolio returns (size), value minus growth decile portfolio returns (value), and micro uncertainty. The details on the construction of micro uncertainty are in Section 2.2. For size and value, we plot the 10-year forward rolling window average from year $t+1$ to year $t+10$ in the left panel, along with micro uncertainty at year t. In the right panel, we plot the low-frequency components of these series, which are obtained after applying the Christiano and Fitzgerald (2003) bandpass filter to isolate frequencies between 25 and 50 years. To facilitate visual comparison, all series are standardized to have mean zero and variance one.

following panel regression:

$$y_{it} = \mu_i + \mu_t + \beta_k k_{it-1} + \beta_n n_{it} + z_{it}, \quad (1)$$

where $y_{i,t}$ is log sales, $k_{i,t-1}$ is lagged value of the log capital stock, $n_{i,t}$ is log number of employees, μ_i is firm fixed effect, and μ_t is time fixed effect. Nominal sales are adjusted to real using the price deflator for gross domestic product. The capital stock is computed using the perpetual inventory method. For the first year, the capital stock is given by total gross property, plant, and equipment plus any net investment, where net investment is the difference between total net property, plant, and equipment and its lagged value. For subsequent years, the capital stock is defined as the sum of its initial value and all subsequent net investments made. Nominal investment is converted to real using the price deflator for nonresidential gross private domestic investment.

We fit the TFP estimated in the previous step to an autoregressive process by running the following panel regression:

$$\hat{z}_{i,t} = \bar{z}_i + \bar{z}_t + \rho_z \hat{z}_{i,t-1} + \hat{\varepsilon}_{i,t}, \quad (2)$$

where $\bar{z}_i$ and $\bar{z}_t$ are firm and time fixed effects. We define the TFP innovations for firm i as the residual $(\hat{\varepsilon}_{i,t})$ of regression Eq. (2).

Micro uncertainty is then constructed annually following Bloom et al. (2018). We compute the cross-sectional interquartile range of firm TFP innovations each year. Micro uncertainty $(\hat{\sigma}_{zt-1})$ is then measured as the linearly detrended time series of the interquartile ranges. Fig. 1 plots micro uncertainty with size and value premia where each series is standardized to have mean zero and variance one in the figure for visual comparison. Size and value premia are computed as 10-year forward rolling averages of the small minus big and the value minus growth extreme decile portfolios, respectively. The left panel plots the raw series, and the right panel plots the low-frequency components of the corresponding series, obtained using the bandpass filter. This figure highlights how micro uncertainty comoves strongly with size and value premia, particularly at low frequencies. When micro uncertainty is high, both size and value strategies are associated with higher risk premia, measured by future realized returns.

Table 1 reports statistics conditional on high versus low micro uncertainty periods to quantify the relation between micro uncertainty and future size and value premia. We define high (low) micro uncertainty periods as years in which micro uncertainty is in the top (bottom) quartile of its distribution. We report return spreads for size and value premia in the top panel. Consistent with the pattern depicted in Fig. 1, we find a stronger size premium in periods of high micro uncertainty. Specifically, small market capitalization firms outperform large ones by 7.54% per year when micro uncertainty is high, but the size premium is negligible in periods of low micro uncertainty. Similarly, the value premium is 7.92% in periods of high micro uncertainty but only 4.50% when micro uncertainty is low. This table also highlights how persistent variation in micro uncertainty can be a source of instability for the size and value premium in short samples.

We also find that micro uncertainty correlates with dispersion in firm fundamentals across size and book-to-market sorted portfolios. In addition to differences in average returns, Table 1 reports average differences in expected payout growth and TFP innovations for the zero-cost small-minus-big and value-minus-growth portfolios conditional on low and micro uncertainty. We compute expected payout growth in Panel B as the average payout growth over the next 10 years, and we find that dividend spread is positive for both size and value long-short portfolios. Small (value) firms have higher future dividend growth rates than big (growth) ones. More importantly, such dividend growth spreads widen in periods of high micro uncertainty, meaning that small (value) firms have even higher future dividend growth rates when micro uncertainty is high.

In the bottom panel of Table 1, we compute average spreads in TFP shocks in the 10 years prior to portfolio formation. All TFP shock spreads reported are negative, meaning that small (value) firms had lower TFP shocks

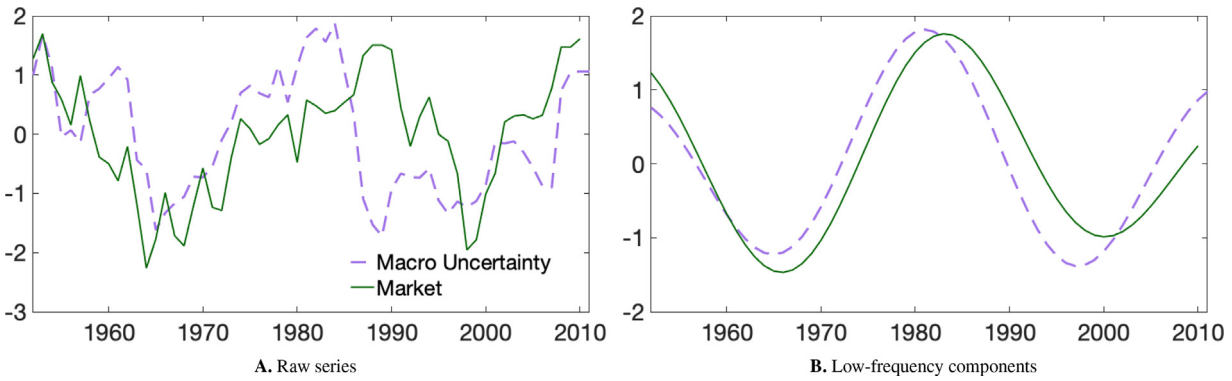

Fig. 2. Macro uncertainty and equity premium.
This figure shows the time series comovement between market excess and macro uncertainty. The details on the construction of macro uncertainty are in Section 2.3. For market excess returns, we plot the 10-year forward rolling window average from year $t+1$ to year $t+10$ in the left panel, along with macro uncertainty at year t. In the right panel, we plot the low-frequency components of these series, which are obtained after applying the Christiano and Fitzgerald (2003) bandpass filter to isolate frequencies between 25 and 50 years. To facilitate visual comparison, all series are standardized to have mean zero and variance one.

prior to portfolio formation than big (growth) ones. This is consistent with small caps and value firms having experienced relatively unfavorable productivity shocks. Interestingly, the TFP spreads between small (value) and big (growth) firms are larger in periods of high micro uncertainty.

As a robustness exercise, we compute other measures of micro uncertainty. Micro uncertainty captures cross-sectional differences in firms' productivity. Alternatively, one can look at cross-sectional dispersion in sales growth rates as an indicator of micro uncertainty. Another possibility is that productivity differences may be reflected in firms' stock market returns. Therefore, cross-sectional dispersion in excess returns is an alternative measure of micro uncertainty. We compute these alternative measures of micro uncertainty and report them in Fig. A.2 in the Appendix. We find that all three measures strongly correlate with each other at both high and low frequencies.

Overall, we find that the average spreads in the value-weighted portfolio future returns, future cash flows, and previous productivity innovations for the size and value strategies are larger when micro uncertainty is high. These empirical patterns are consistent with our model, which we will discuss in Section 3.

2.3. Macro uncertainty

We define macro uncertainty as the time-series standard deviation of output growth. To this end, we first compute the standard deviation of output growth using a backward 20-quarter rolling sample:

$$\hat{\sigma}_s = \sqrt{\frac{1}{20-1}\sum_{j=s-19}^{s}(\Delta\hat{y}_j - \Delta\bar{y}_s)^2}, \tag{3}$$

where the index s is in quarters, $\Delta\hat{y}_s$ is quarterly log output growth, and $\Delta\bar{y}_s$ is the average in the backward 20-quarter rolling sample. We compute macro uncertainty in each year. Fig. 2 plots macro uncertainty with the equity premium. The equity premium is calculated each year as the 10-year forward rolling average of the market portfolio return minus the riskfree rate. The left panel displays the raw series, while the right panel shows the corresponding low-frequency components obtained using the bandpass filter. This figure shows that the positive relation between macro uncertainty and the equity premium is enhanced at low frequencies. Fig. A.3 in the Appendix shows that macro uncertainty measures constructed using other aggregate growth rates (e.g., consumption or TFP) are highly correlated with each other and with the market premium at both high and low frequencies.

Figs. 1 and 2 highlight the tight link between measures of uncertainty and risk premia. We have shown that micro uncertainty covaries strongly with both size and value premia, while macro uncertainty covaries with the market risk premium. Next, we document that our uncertainty measures feature a strong negative correlation with one another at low frequency (see the left panel of Fig. 3). Additionally, the right panel of Fig. 3 shows that the low-frequency component of the equity premium is negatively related to the low-frequency components of size and value premia, suggesting that the market factor is a good long-run hedge to the size and value factors. In the next section, we formally quantify and assess the statistical significance of the low-frequency correlations depicted in Figs. 1, 2, and 3.

2.4. Low-Frequency correlations

This section describes the long-run correlations between the aggregate and cross-sectional measures of risk. Table 2 reports the correlations between the low-frequency components of the size premium, value premium, equity premium, micro uncertainty, and macro uncertainty. The low-frequency components are obtained using the bandpass filter and isolating frequencies between 25 and 50 years. Table A.1 in the Appendix reports the long-run correlations of these series using different frequency ranges. The correlation patterns are robust to alternative frequencies with a lower cutoff of 8, 20, and 25 years and

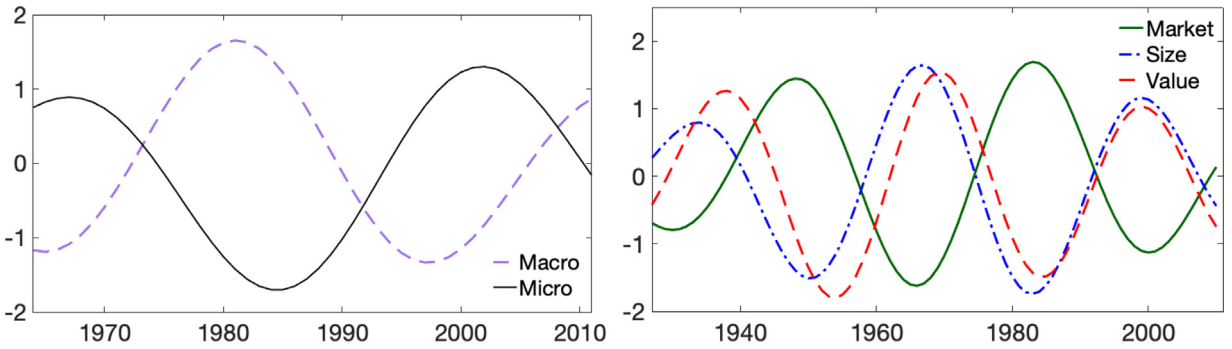

Fig. 3. Aggregate and cross-sectional risk.
This figure shows the time series comovement between the low-frequency component following variables: macro and micro uncertainty, and market, size, and value premia. For market risk premium, we compute a 10-year forward rolling window average excess return from year $t+1$ to year $t+10$. Similarly, for size and value, we compute a 10-year forward rolling window average from year $t+1$ to year $t+10$ of zero-cost small-minus-big and value-minus-growth portfolios. The details on the construction of micro and macro uncertainty are in Sections 2.2 and 2.3. To obtain the low-frequency components of these series, we apply the Christiano and Fitzgerald (2003) bandpass filter to isolate frequencies between 25 and 50 years. In the left panel, we plot the low-frequency components of both micro and macro uncertainty. In the right panel, we plot low-frequency components of the market, size, and value premia. To facilitate visual comparison, all series are standardized to have mean zero and variance one.

an upper cutoff of 50 and 75 years. The top panel of Table A.1 shows that the raw correlations have the same sign as the low-frequency correlations.

The magnitude of the correlation in Table 2 verifies the strong relations depicted in Figs. 1, 2, and 3. The low-frequency series are persistent over time, so standard correlation t-statistics are not the appropriate test due to the short length of the time series. To address this issue, we conduct two distinct empirical exercises to assess the correlations' statistical significance. First, we compute block-bootstrapped standard errors. Second, we formally reject a null hypothesis of zero correlation.

The first exercise computes block-bootstrapped standard errors, reported in Column (2) of Table 2. We bootstrap the sample in blocks of 35 years to capture the low-frequency patterns isolated using the bandpass filter. We truncate each resampled data series to be the same length as the original data. Then, we apply the bandpass filter to resampled data and compute correlations between these low-frequency components. We resample the data 100,000 times and compute the standard errors of the estimated low-frequency correlations. The bootstrapped standard errors suggest that all the correlation coefficients estimated are statistically significant.

The second procedure tests the null hypothesis that the pairwise correlations between the low-frequency components are zero. We assume that the low-frequency series are serially autocorrelated, but they are uncorrelated under the null. We compute the first-order autocorrelation coefficient for each low-frequency series and generate simulated data for $10,000+T$ periods, assuming that each data series follows an AR(1) process, where T is our data length. We compute the correlation between the simulated series using only the last T observations. We repeat these steps 100,000 times and compute the simulated p-value based on all simulated data (i.e., the fraction of simulations with correlations as extreme as those observed in the data), reported in Column (3) of Table 2. We reject the null of zero correlation with at least 5% confidence for each estimated coefficient.

Both empirical exercises—bootstrapping standard errors and hypothesis testing using simulated data—confirm that all low-frequency correlations are statistically significant. Moreover, the magnitudes are large as they range from 0.77 to 0.99 in absolute value.

3. Model

This section presents an investment-based asset pricing model featuring heterogeneous firms cast in partial equilibrium. A representative agent is assumed to have recursive preferences defined over aggregate consumption. Consumption growth is exogenously specified to include a persistent conditional mean with stochastic volatility, capturing fluctuating macro uncertainty. Competitive firms use capital as the only input to produce a homogeneous good and incur fixed and proportional operating costs. Firm productivity contains an aggregate and a firm-specific component. The aggregate component is exposed to long-run consumption risks. The firm-specific component is specified as an autoregressive process with stochastic volatility to capture fluctuating micro uncertainty. The micro and macro uncertainty processes contain a common low-frequency component that affects the two uncertainty processes in the opposite direction, as documented in Section 2. Each firm accumulates capital subject to quadratic capital adjustment costs.

3.1. Pricing kernel

The representative agent has lifetime utility, U_t, defined recursively over aggregate consumption, C_t, as:

$$U_t = \left[(1-\beta) C_t^{1-\frac{1}{\psi}} + \beta \left(E_t \left[U_{t+1}^{1-\gamma} \right] \right)^{\frac{1-1/\psi}{1-\gamma}} \right]^{\frac{1}{1-1/\psi}}, \tag{4}$$

where β is the time discount factor, ψ is the intertemporal elasticity of substitution, and γ is the coefficient of relative risk aversion (Epstein and Zin, 1989). The corresponding stochastic discount factor is given by:

$$M_{t+1} = \beta\left(\frac{C_{t+1}}{C_t}\right)^{-\frac{1}{\psi}}\left(\frac{U_{t+1}^{1-\gamma}}{E_t\left[U_{t+1}^{1-\gamma}\right]}\right)^{\frac{1/\psi-\gamma}{1-\gamma}}. \tag{5}$$

Log consumption growth, defined as $\Delta c_{t+1} \equiv \log(C_{t+1}/C_t)$, evolves exogenously and is specified as in Bansal and Yaron (2004):

$$\Delta c_{t+1} = \mu + x_t + \sigma_t \varepsilon_{ct+1}, \quad \varepsilon_{ct+1} \sim \text{i.i.d. } \mathcal{N}(0,1), \tag{6}$$

$$x_{t+1} = \rho_x x_t + \sigma_x \sigma_t \varepsilon_{xt+1}, \quad \varepsilon_{xt+1} \sim \text{i.i.d. } \mathcal{N}(0,1), \tag{7}$$

where the two shocks, ε_{ct+1} and ε_{xt+1}, are uncorrelated. Long-run consumption risks are captured by the persistent autoregressive term, x_t. Fluctuating macro uncertainty is captured by the time-varying volatility process of consumption growth, σ_t:

$$\sigma_t = \bar{\sigma} + \varsigma \nu_t, \tag{8}$$

$$\nu_t = \rho_\nu \nu_{t-1} + \sigma_\nu \varepsilon_{\nu t}, \ \varepsilon_{\nu t} \sim \text{i.i.d. } \mathcal{N}(0,1), \tag{9}$$

where ν_t is the common low-frequency component in micro and macro uncertainty that affects the two types of uncertainty in opposite directions. The parameter ς captures the sensitivity of macro uncertainty to the process ν_t. The specification of micro uncertainty in the model is described in Section 3.2 below. The volatility shock, $\varepsilon_{\nu t}$, is assumed to be uncorrelated with the level shocks to consumption growth.

3.2. Firms

Competitive firms take prices as given and produce a homogeneous good using capital. Firm productivity is subject to aggregate and firm-specific shocks. There are no manager-shareholder conflicts and the firms are all-equity financed. Output, Y_{it}, of firm i is produced using decreasing returns to scale technology with capital, K_{it}, as the only factor input:

$$Y_{it} = A_{it}^{1-\alpha} K_{it}^{\alpha}, \tag{10}$$

where $\alpha > 0$ is the curvature parameter and A_{it} is the total factor productivity of firm i. Operating profits are defined as:

$$\Pi_{it} \equiv Y_{it} - f_{it} \cdot Z_{t-1}, \tag{11}$$

where operating costs, f_{it}, contain both a constant and linear component proportional to the capital stock: $f_{it} \equiv \tilde{f} + f\hat{K}_{it}$, where $\hat{K}_{it} \equiv K_{it}/Z_{t-1}$. The costs are scaled by the aggregate trend so the costs do not become trivially small along the balanced growth path.

Measured TFP, $A_{it} \equiv Z_t Z_{it}$, consists of an aggregate component, Z_t, and a firm-specific component, Z_{it}. The aggregate component has a levered exposure to the long-run consumption growth risks component, x_t:

$$\log(Z_t/Z_{t-1}) \equiv \mu + \phi x_t, \tag{12}$$

where $\phi \geq 1$ is the leverage parameter. The log of the firm-specific component, $z_{it} \equiv \log(Z_{it})$, evolves as:

$$z_{it+1} = \rho_z z_{it} + \sigma_{zt}\varepsilon_{it+1}, \quad \varepsilon_{it+1} \sim \text{i.i.d. } \mathcal{N}(0,1), \tag{13}$$

where the shock ε_{it+1} is uncorrelated with all aggregate shocks. The firm-specific productivity shocks are uncorrelated between any two different firms (i.e., $corr(\varepsilon_{it+1}, \varepsilon_{jt+1}) = 0, \ \forall i \neq j$). Fluctuating micro uncertainty, σ_{zt}, is common across all firms and modeled as:

$$\sigma_{zt} = \bar{\sigma}_z + \varsigma_z \nu_t, \tag{14}$$

where ν_t is the common low-frequency component in micro and macro uncertainty specified above in Eq. (9) and ς_z governs the sensitivity of micro uncertainty to the process ν_t.

At time t, firm i makes an investment, I_{it}, to the capital stock, K_{it+1}, next period. The capital accumulation equation is given by:

$$K_{it+1} = (1-\delta)K_{it} + I_{it}, \tag{15}$$

where δ is the rate of depreciation. Real investment frictions are captured by an asymmetric capital adjustment cost function with a linear and quadratic component as in Bai et al. (2019):

$$H\left(\frac{I_{it}}{K_{it}}\right) = \begin{cases} a^+ K_{it} + \frac{\theta^+}{2}\left(\frac{I_{it}}{K_{it}}\right)^2 K_{it} & \text{for } I_{i,t} > 0 \\ 0 & \text{for } I_{it} = 0 \\ a^- K_{it} + \frac{\theta^-}{2}\left(\frac{I_{it}}{K_{it}}\right)^2 K_{it} & \text{for } I_{i,t} < 0 \end{cases} \tag{16}$$

where the parameter restrictions $a^- > a^+ > 0$ and $\theta^- > \theta^+ > 0$ capture partial investment irreversibility. The source of funds constraint of the firm is:

$$D_{it} = \Pi_{it} - I_{it} - H\left(\frac{I_{it}}{K_{it}}\right), \tag{17}$$

where D_{it} are net firm payouts.

The firms take the stochastic discount factor, M_{t+1}, as given and $\mathbf{S}_{it} \equiv (K_{it}, Z_{it}, x_t, \nu_t)'$ is a vector collecting the firm-specific and aggregate state variables. Firm i maximizes the market value of equity, V_{it}, by choosing optimal investment, I_{it}, and an optimal exit decision:

$$V_{it} \equiv V_{it}(\mathbf{S}_{it}) = \max\left\{\max_{I_{it}} D_{it} + E_t[M_{t+1}V_{it+1}(\mathbf{S}_{it+1})], sK_{it}\right\}, \tag{18}$$

subject to the capital accumulation equation and the source of funds constraint. The parameter $s > 0$ governs the liquidation value of capital. When $\max_{I_{it}} D_{it} + E_t[M_{t+1}V_{it+1}(\mathbf{S}_{it+1})] \geq sK_{it}$, firm i remains in operation.

When $\max_{I_{it}} D_{it} + E_t[M_{t+1}V_{it+1}(\mathbf{S}_{it+1})] < sK_{it}$, firm i exits at the start of time t. Following Bai et al. (2019), the stock return of the exiting firm, R_{it}, is set to a constant delisting return, $\tilde{R}$. The firm enters an instantaneous reorganization process immediately upon making the exit decision at the beginning of time t. The current shareholders of the firm receive the liquidation value of capital, sK_{it}. New shareholders take over the remainder of the firm's capital, $(1-s-\kappa)$, where $\kappa \in [0, 1-s]$ captures reorganization costs. A new firm replaces the exiting firm at the beginning of t with an initial capital stock of $(1-s-\kappa)K_{it}$ and productivity is drawn from the cross-sectional distribution of z_{it}.

Table 1
Size and value premia conditional on micro uncertainty.
This table reports average future returns, future dividend growth rates, and TFP spread prior to portfolio formations. Panel A reports the average future returns of size and value strategies over 10 subsequent years in high and low micro uncertainty periods. The details on the construction of micro uncertainty are in Section 2.2. We define high (low) micro uncertainty periods as years in which micro uncertainty is in the top (bottom) quartile of its distribution. The size strategy is a zero-cost portfolio long on the bottom decile based on market capitalization and short on the top decile. The value strategy is a zero-cost portfolio long on the highest decile based on book-to-market and short on the bottom decile. In Panels B and C, we compute the average dividend growth rates and the average spread in TFP between the extreme portfolio deciles. TFP is computed as the average TFP innovation over the 10-year window up to the portfolio formation date. Return and dividend growth spread are 10-year forward rolling window averages. The return data is from Ken French's website, while the dividend growth rate and TFP are from Compustat. The sample is from 1964 to 2020 at an annual frequency. We report annualized averages and Newey-West corrected t-statistics.

	Size		Value	
	Low Micro Uncertainty (1)	High Micro Uncertainty (2)	Low Micro Uncertainty (3)	High Micro Uncertainty (4)
Panel A: Returns Spread				
Avg.	−0.28	7.54	4.50	7.92
t-stat.	−0.15	5.60	1.82	3.27
Panel B: Dividend growth spread				
Avg.	6.17	8.49	4.98	7.02
t-stat.	3.53	8.59	2.91	4.62
Panel C: Average spread in TFP shocks				
Avg.	−2.65	−2.96	−2.12	−2.72
t-stat.	−6.81	−6.29	−8.23	−3.80

4. Quantitative analysis

This section presents the quantitative assessment of the model. We explain how the model can explain the novel long-run trends in the size, value, and market strategy returns documented in Section 2.

4.1. Calibration

We calibrate our model at a monthly frequency and report calibrated parameters in Table 3. The parameters governing preferences and the consumption growth process are set to standard values in the long-run risks literature, reported in Panel A. The intertemporal elasticity of substitution, ψ, is set to 1.5, the coefficient of relative risk aversion, γ, to 11, and the subjective discount factor, β, to 0.997. This parameter restriction, $\psi > 1/\gamma$, implies that the representative household has a preference for an early resolution of uncertainty and is averse to persistent consumption growth risks.

The parameters related to technology and adjustment costs are reported in Panel B. The curvature parameter of the production function, α, is set to 0.3, close to the estimated value in Gomes (2001). The monthly capital depreciation rate, δ, of 0.01 matches the findings of an annual rate of 12% from Cooper and Haltiwanger (2006). The leverage parameter, ϕ, which governs the sensitivity of productivity growth to long-run risks, is set to a value of 3, which is also in line with the dividend leverage parameter from Bansal and Yaron (2004). The fixed and proportional operating cost parameters, $\tilde{f}$ and f, and the adjustment cost parameters, a^+, a^-, θ^+, and θ^-, are calibrated to fit the properties of the book-to-market and market cap deciles. The role of these costs is then examined in Section 4.5 through extensive comparative statics exercises reported in Table 11. The delisting return, $\tilde{R}$, follows the CRSP estimate by Hou et al. (2020). The reorganization cost parameter κ and the liquidation parameter s are calibrated to the values in Bai et al. (2019).

Panel C reports the parameters governing the level shocks. The parameter, μ, is set to match the per capita growth rate. The parameters ρ_x and σ_x are calibrated to be consistent with the low-frequency growth cycle dynamics from Kung and Schmid (2015). The persistence of the firm-specific TFP shocks, ρ_z, is set to 0.97 as in Bai et al. (2019).

4.1.1. Uncertainty processes

Panel D reports the parameters governing the micro and macro uncertainty processes. We first measure the common low-frequency uncertainty process by calculating the first principal component (*PC1*) of the low-frequency micro and macro uncertainty series, assuming that it affects micro uncertainty positively and macro uncertainty negatively. The series is standardized to mean zero and unit variance. We find that *PC1* explains 88.5% of the total variance of the low-frequency micro and macro uncertainty series. We choose parameter values for the common low-frequency uncertainty process in the model, ν_t, to match the persistence and volatility of *PC1* by setting $\rho_\nu = 0.98$ and $\sigma_\nu = 0.02$, respectively.

We calibrate the parameter ($\varsigma = 0.002$) governing the sensitivity of macro uncertainty to the common low-frequency uncertainty component to be consistent with the low-frequency volatility of macro uncertainty. The parameter $\bar{\sigma} = 0.004$ is set to match the average level of macro uncertainty. We set the absolute value of the parameter $\varsigma_z = -0.35$ to align with the low-frequency volatility of micro uncertainty. The negative sign is needed to explain the low-frequency correlation of micro and macro uncertainty (documented in Section 2.4 and explored in the model in Section 4.4). The parameter $\bar{\sigma}_z$ matches the average level of micro uncertainty. Panel A of Table 4 re-

Table 2
Low-frequency correlations.
This table reports low-frequency correlations between market risk, size and value risk premia, and both micro and macro uncertainty. For market risk premium, we compute a 10-year forward rolling window average excess return from year $t+1$ to year $t+10$. Similarly, for size and value, we compute a 10-year forward rolling window average from year $t+1$ to year $t+10$ of zero-cost small-minus-big and value-minus-growth portfolios. The details on the construction of micro and macro uncertainty are in Sections 2.2 and 2.3. To obtain the low-frequency components of these series, we apply the Christiano and Fitzgerald (2003) band-pass filter to isolate frequencies between 25 and 50 years. In Column (1), we report the correlation between the low-frequency component of these series. In Column (2), we report bootstrapped standard errors. We bootstrap the sample in blocks with a length of 35 years and apply the band-pass filter to re-sampled data. We truncate each re-sampled data series to be the same length as the original data, then compute the correlations between the low-frequency components. We re-sample the data 100,000 times and compute the standard errors of the estimated low-frequency correlations. In Column (3), we report p-values from simulated data under the null hypothesis of no correlation between the low-frequency components. Specifically, we assume that the low-frequency series are serially autocorrelated but are uncorrelated with each other. We compute the first-order autocorrelation coefficient for each low-frequency series and generate simulated data for $10,000+T$ periods, assuming that each data series follows an AR(1) process, where T is our data length. We compute the correlation between the simulated series using only the last T observations. We repeat these steps 100,000 times and compute the simulated one-sided p-value based on all simulated data, i.e., the fraction of simulations with correlations as extreme as those observed in the data.

	Coefficient (1)	Bootstrapped Standard Error (2)	p-value from simulated data (3)
Corr (Size, Value)	0.94	0.04	0.000
Corr (Size, Market)	−0.99	0.02	0.000
Corr (Value, Market)	−0.91	0.04	0.001
Corr (Size, Micro)	0.92	0.09	0.001
Corr (Value, Micro)	0.86	0.10	0.009
Corr (Market, Micro)	−0.95	0.07	0.000
Corr (Size, Macro)	−0.91	0.14	0.002
Corr (Value, Macro)	−0.77	0.27	0.031
Corr (Market, Macro)	0.88	0.10	0.005
Corr (Micro, Macro)	−0.77	0.19	0.035

Table 3
Calibration.
This table reports the parameter values of the model which are calibrated at monthly frequency. Panel A reports the preference parameters, Panel B details the production parameters, Panel C reports the parameters of governing the level shocks, and Panel D outlines the parameters related to the uncertainty shocks.

Parameter	Description	Model
Panel A: Stochastic Discount Factor		
β	Time discount factor	0.997
γ	Relative risk aversion coefficient	11
ψ	Intertemporal elasticity of substitution	1.5
Panel B: Firms		
α	Curvature parameter in the production function	0.3
δ	Rate of capital depreciation	0.01
ϕ	Leverage of productivity growth	3
$\tilde{f}$	Fixed operating costs	0.36
f	Proportional operating costs	0.70
θ^-, a^-	Downward capital adjustment costs	350, 3
θ^+, a^+	Upward capital adjustment costs	300, 0
$\tilde{R}$	Delisting return	0.85
κ	Reorganization costs	0.25
s	Liquidation value	0
Panel C: Level Shocks		
μ	Average growth rate	1.90%/12
ρ_x	Persistence of log aggregate productivity	0.985
σ_x	Volatility scaling of log aggregate productivity	0.13
ρ_z	Persistence of log firm-specific productivity	0.97
Panel D: Uncertainty Shocks		
ρ_ν	Persistence of common uncertainty	0.98
σ_ν	Volatility of common uncertainty	0.02
ς	Macro uncertainty loading	0.002
$\bar{\sigma}$	Level of macro uncertainty	0.004
ς_z	Micro uncertainty loading	−0.35
$\bar{\sigma}_z$	Level of micro uncertainty	0.1

Table 4
Summary statistics.
This table reports the average, volatility, and volatility of the low-frequency component (i.e., low-frequency volatility) of the market, size and value premia, real risk-free rate, micro uncertainty, and macro uncertainty. Columns 2, 3, and 4 refer to moments from the data, while Columns 5, 6, and 7 refer to their counterparts in the model. The details on the construction of micro and macro uncertainty are in Sections 2.2 and 2.3. For market risk premium, we compute a 10-year forward rolling window average excess return from year $t+1$ to year $t+10$. Similarly, for size and value, we compute a 10-year forward rolling window average from year $t+1$ to year $t+10$ of zero-cost small-minus-big and value-minus-growth portfolios. The real risk-free rate of return is obtained by subtracting realized inflation based on Fred's Consumer Price Index (All Urban Consumers: All Items in U.S. City Average). We obtain the low-frequency components of these series by applying the band-pass filter to isolate frequencies between 25 and 50 years. The sample period for equity and the risk-free rate of return data is from 1926 to 2021. Micro uncertainty data is from 1964 to 2020 at an annual frequency. Macro uncertainty data is from 1952 to 2020 at an annual frequency. For the model moments, we compute averages and standard deviations across 500 simulations, each with a length of 100 years. Each moment from the model is constructed akin to its data counterpart.

	Data			Model		
Variable	average	volatility	low-frequency volatility	average	volatility	low-frequency volatility
(1)	(2)	(3)	(4)	(5)	(6)	(7)
Panel A: micro and macro uncertainty						
Micro Uncertainty	12.53	1.76	0.33	12.66	0.92	0.31
Macro Uncertainty	0.86	0.37	0.16	0.86	0.47	0.18
Panel B: size premium, value premium, equity premium, and real risk-free rate of return						
Equity premium	8.32	18.50	3.51	9.98	15.65	1.77
Size premium	5.73	25.22	4.82	4.76	11.94	2.46
Value premium	5.11	22.03	3.31	4.15	10.63	2.15
Riskfree rate	0.62	1.40	0.42	2.98	0.56	0.24

ports the summary statistics for micro and macro uncertainty both in the model and data.[3]

4.2. Unconditional risk premia

This section describes the model mechanisms for generating realistic unconditional aggregate and cross-sectional risk premia. Panel B of Table 4 reports the mean, volatility, and low-frequency volatility of the annualized equity, size, and value premia along with the riskfree rate from the model and data. The low-frequency volatility is the standard deviation of the long-run component obtained using the bandpass filter described in Section 2.

Using a log-linear approximation only to highlight intuition (reported model results are computed using a global solution method described in Appendix C), expected return spreads between two firms can be expressed as:

$$E[r_{jt} - r_{it}] = (\beta_j - \beta_i)'\lambda, \tag{19}$$

where $\lambda = [\lambda_x \ \lambda_w]'$ is the 2x1 vector containing the market prices of long-run risks and macro uncertainty risks, respectively, and $\beta_j = [\beta_{xj} \ \beta_{wj}]'$ is the corresponding 2x1 vector of the factor exposures of firm j's returns to each source of risk, where $j \neq i$. Appendix B provides details of the derivations above. As the market price of risk for long-run risks is quantitatively most important, differences in unconditional betas on long-run risks across claims are the main determinant of unconditional risk premia in our model.

The TFP shock structure directly influences the risk exposures of firms to long-run risks. The measured TFP growth of firm i is given by:

$$\frac{A_{it+1}}{A_{it}} = \frac{Z_{it+1}}{Z_{it}} \cdot e^{\mu + \phi x_{t+1}}, \tag{20}$$

where Z_{it+1} is the firm-specific component of productivity and x_{t+1} is long-run consumption risks. Equation (20) illustrates how the growth rate of Z influences the firm-specific cash flow exposures to long-run risks via productivity. The investment frictions are then paramount to prevent the firms from offsetting these risk exposures through their investment decisions. We discuss next how the shock structure and investment frictions determine the cash flow exposures in equilibrium across characteristics, leading to positive size and value premia.

Mean reversion in the firm-specific productivity shock helps to produce a size effect (e.g., Babenko et al., 2016; Clementi and Palazzo, 2019). Small market cap (small) firms in our model are characterized by a small capital stock and low Z today. Due to mean reversion in Z, the future growth rate of Z is expected to be high, exposing the cash flows of small firms more to long-run risks. Small firms also have limited capital stock that they can liquidate to hedge bad aggregate shocks. Higher disinvestment costs from the asymmetric quadratic cost specification further strengthen their high cash flow exposure to long-run risks. In contrast, large market cap (big) firms have large capital stock and high Z. Mean reversion in Z implies that big firms have low exposure to long-run risks through their productivity, while the large capital stock allows big firms to hedge bad aggregate shocks, reinforcing the low cash flow exposure to long-run risks.

Panel A of Fig. 4 provides a visual depiction of these time-series model dynamics for the benchmark model at calibrated parameters. We plot productivity and payouts in the one year before and after portfolio formation for the small (solid blue line) and big (dotted red line) decile port-

[3] We truncate negative observations for both uncertainty processes to a small positive number. These negative observations occur with less than 0.2% for micro uncertainty and less than 0.01% for macro uncertainty.

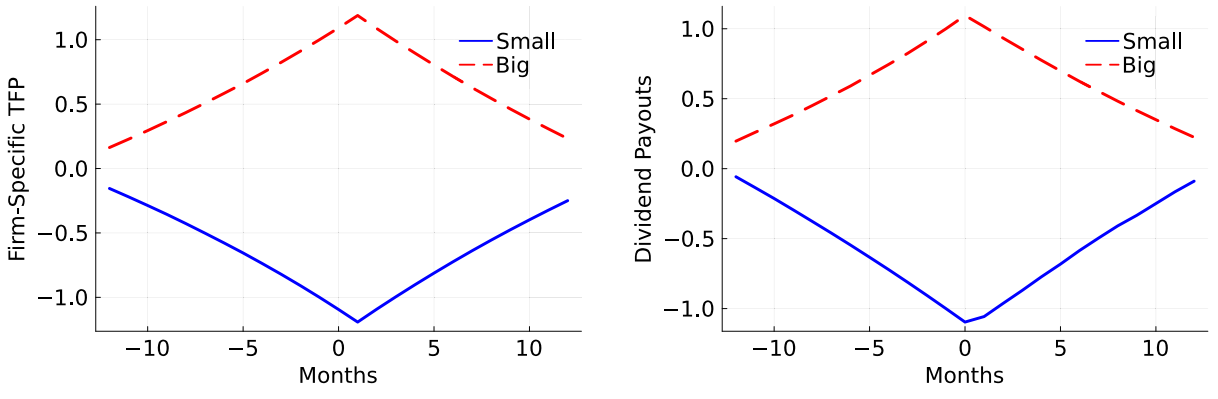

A. TFP and payout dynamics for size-sorted portfolios

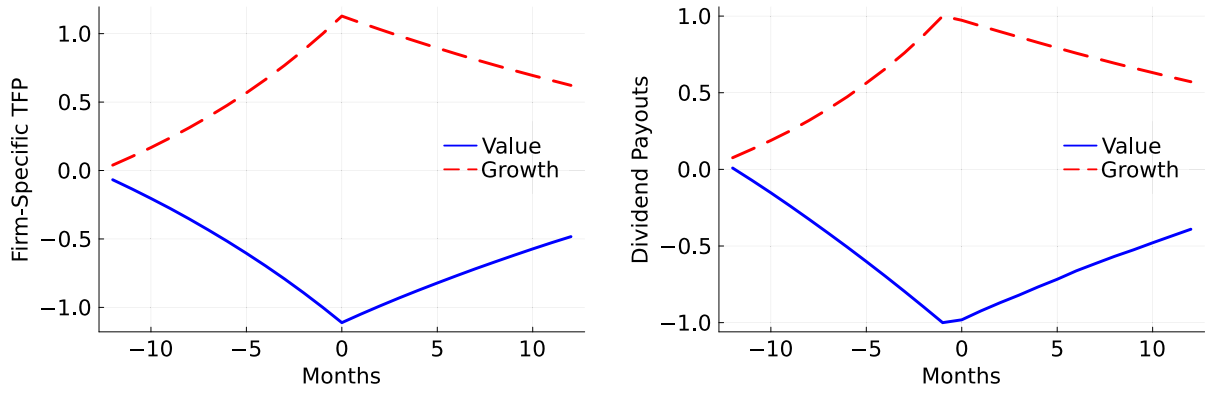

B. TFP and payout dynamics for *B/M*-sorted portfolios

Fig. 4. Model: Portfolio formation.
This figure shows the standardized time series of the average characteristics within portfolio deciles one and ten. In month zero, firms are sorted into decile portfolios on either size (Panel A) or book-to-market (Panel B). Holding the portfolio allocation of firms constant, the figure plots the average time-series dynamics from one year before portfolio formation until one year after portfolio formation. Panel A shows the dynamics for firm-specific TFP and dividend payout for small firms (solid blue) and big firms (dotted red). Panel B shows the average firm characteristics for value firms (solid blue) and growth firms (dotted red). (For interpretation of the references to colour in this figure legend, the reader is referred to the web version of this article.)

folios. As the cash flows of small firms are more exposed to long-run risks than big firms, small firms command higher expected returns in equilibrium. In Appendix B, we analytically show a negative relation between market cap and exposure to long-run risks in the case of fixed capital. Empirical evidence supporting the cash flow exposures to long-run risks across size-sorted portfolios is presented in Section 4.3.2.[4]

Table 5 reports the mean and corresponding t-stat of annualized value-weighted returns, payout growth, and TFP (as a percentage of average TFP) across the size deciles. To calculate the model moments, we conduct 500 simulations, each with 1000 firms and 100 years worth of simulated data. The model quantitatively reproduces the strong negative relation between size and expected returns across the deciles. Consistent with the time-series model dynamics described above, we find that size is negatively related to expected payout growth and positively related to current TFP in the cross-section. Altogether, we find strong empirical support for the model explanation of the size premium.

Operating leverage and asymmetric capital adjustment costs contribute to a positive value premium (e.g., Zhang, 2005; Donangelo, 2016). Value (i.e., high book-to-market) firms are characterized by low productivity but burdened with large and unproductive capital stock, implying a very low marginal product of capital, $MPK_{it} \equiv \alpha(A_{it}/K_{it})^{1-\alpha}$. The low Z today implies that the measured TFP of value firms are more exposed to long-run risks due to mean reversion. The low MPK induces strong incentives to liquidate capital (and hedge long-run risks) but is muted by the high disinvestment costs. The operating costs proportional to the capital stock prevent value firms from making large payouts today, ensuring their high cash flow exposure to long-run risks. Growth (i.e., low book-to-market) firms are associated with high Z but have small capital stock, implying a very high MPK. High Z means lower exposure to long-run risks through TFP, but the high MPK implies strong incentives to accumulate capital which increases exposure to long-run risk. Capital adjustment costs help to prevent growth firms from investing aggressively to reinforce their low cash flow exposure to long-run risks.

[4] Mirroring our evidence of low-frequency aggregate risk exposures, Crouzet and Mehrotra (2020) also find that the cash flows of small firms vary more with business cycle risks using census data.

Table 5
Size-sorted portfolios.
This table reports average excess returns and dividend growth rates of size-sorted portfolios. Panel A refers to moments from the data, while Panel B refers to their counterparts in the model. Stocks are sorted into ten deciles based on market equity (NYSE breakpoints). Portfolios are rebalanced annually at the end of June. We report annualized averages, annualized standard deviations, and t-statistics for excess returns and dividend growth rates of each decile portfolio, as well as the equal-weighted average of total factor productivity (TFP) innovation at portfolio formation. We report the spread between top and bottom deciles in Column 11 (small minus big). The dividend growth rate is computed from cum- and ex-dividend returns as detailed in Appendix A.1. TFP innovations for each firm are computed as described in Section 2.2, and it is the residual from the panel regression specified by Eq. (2). For each portfolio bin, we compute the average TFP innovation in the year immediately prior to the portfolio formation date. In Panel A, we report these statistics from data; in Panel B, we report the same statistics implied by our calibrated model. The return data is from Ken French's website, while the dividend growth rate and TFP are from CRSP and Compustat. The sample period for returns and dividend growth rates is from 1926 to December 2021. For TFP, the sample is from 1964 to 2020 at an annual frequency. For the model moments in Panel B, we compute averages and standard deviations across 500 simulations, each with a length of 100 years. Each moment from the model is constructed akin to its data counterpart.

	Small (1)	(2)	(3)	(4)	(5)	(6)	(7)	(8)	(9)	Big (10)	Spread (11)
Panel A: Data											
Returns											
Avg.	13.52	12.17	11.94	11.39	10.90	10.98	10.27	9.94	9.09	7.79	5.73
Std.	34.01	30.15	27.44	25.74	24.34	23.47	22.22	21.17	20.02	17.46	25.22
t-stat.	3.88	3.94	4.25	4.32	4.37	4.57	4.51	4.59	4.43	4.36	2.22
Dividend Growth											
Avg.	9.58	10.09	8.75	7.33	8.39	6.76	5.59	5.74	4.51	2.66	6.91
Std.	42.70	38.28	34.73	27.23	31.44	26.79	20.24	24.20	20.50	17.31	42.06
t-stat.	2.16	2.54	2.43	2.59	2.57	2.43	2.66	2.29	2.12	1.48	1.58
TFP											
Avg.	−1.58	−0.63	0.03	−0.09	0.48	0.60	0.40	0.65	0.66	0.92	−2.49
Std.	1.79	1.38	1.38	1.59	1.18	1.55	1.40	1.27	1.49	2.11	3.31
t-stat.	−6.66	−3.46	0.16	−0.45	3.06	2.95	2.14	3.83	3.35	3.29	−5.69
Panel B: Model											
Returns											
Avg.	13.16	12.31	11.78	11.32	11.14	10.76	10.18	9.84	9.33	8.40	4.76
Std.	24.26	20.95	19.61	18.71	17.99	17.34	16.75	16.12	15.42	14.29	11.94
t-stat.	4.51	5.90	6.19	6.34	6.49	6.44	6.24	6.11	5.89	5.51	2.42
Dividend Growth											
Avg.	12.17	12.42	10.76	8.92	7.12	5.44	3.87	2.36	0.91	−0.78	12.95
Std.	29.63	32.08	31.50	30.35	28.95	27.51	26.07	24.56	23.05	21.56	36.66
t-stat.	4.13	3.89	3.43	2.95	2.46	1.98	1.49	0.96	0.39	−0.36	3.55
TFP											
Avg.	−1.46	−0.88	−0.57	−0.32	−0.10	0.11	0.33	0.57	0.88	1.48	−2.94
Std.	0.50	0.31	0.20	0.13	0.07	0.07	0.13	0.21	0.31	0.51	1.00
t-stat.	−7.41	−7.21	−7.10	−7.03	−5.82	5.95	6.83	7.06	7.15	7.22	−7.33

Panel B of Fig. 4 illustrates the productivity and payout dynamics of the value and growth portfolio in the benchmark model. These cash flow dynamics imply that value firms are more exposed to long-run risks than growth firms, leading to a positive value premium. We analytically show the positive link between book-to-market and exposure to long-run risks in the case of fixed capital in Appendix B. Section 4.3.2 provides empirical support for the conditional long-run risk exposures across book-to-market-sorted portfolios.

Table 6 reports the mean and corresponding t-stat of annualized value-weighted returns, payout growth, and TFP (as a percentage of average TFP) across the book-to-market deciles. The model quantitatively replicates the strong positive relation between book-to-market and expected returns across the deciles. Consistent with model dynamics, we find that book-to-market is positively related to expected payout growth and negatively related to current TFP in the cross section. In sum, we find broad empirical support for the model explanation of the unconditional size and value premium.

The presence of persistent consumption risks generates a strong precautionary savings motive to explain the low average riskfree rate. Aggregate dividends are exposed to long-run risks through productivity (e.g., Gomes et al. (2009), Croce (2014), and Kung and Schmid (2015)), generating a large and positive equity premium as in Bansal and Yaron (2004). The model provides a good general fit of the first and second moments of the size, value, and equity premium, which are summarized in Panel B of Table 4. We study the conditional dynamics of risk premia next, which is the focal point of this paper.

4.3. Conditional risk premia

This section outlines how the joint dynamics of micro and macro uncertainty can rationalize the low-frequency trends in the returns to size, value, and market strategies. Using a log-linear approximation only for illustrative purposes, the conditional cross-sectional risk premium can be expressed as:

$$E_t[r_{jt+1} - r_{it+1}] = (\beta_{jt} - \beta_{it})'\lambda_t, \tag{21}$$

Table 6
Book-to-market sorted portfolios.
This table reports average excess returns and dividend growth rates of book-to-market-sorted portfolios. Panel A refers to moments from the data, while Panel B refers to their counterparts in the model. Stocks are sorted into ten deciles based on book-to-market ratios (NYSE breakpoints). Portfolios are rebalanced annually at the end of June, using the book-to-market ratio from the previous year. We report annualized averages, annualized standard deviations, and t-statistics for excess returns and dividend growth rates of each decile portfolio, as well as the equal-weighted average of total factor productivity (TFP) innovation at portfolio formation. We report the spread between top and bottom deciles in Column 11 (value minus growth). The dividend growth rate is computed from cum- and ex-dividend returns as detailed in Appendix A.1. TFP innovations for each firm are computed as described in Section 2.2, and it is the residual from the panel regression specified by Eq. (2). For each portfolio bin, we compute the average TFP innovation in the year immediately prior to the portfolio formation date. In Panel A, we report these statistics from data; in Panel B, we report the same statistics implied by our calibrated model. The return data is from Ken French's website, while the dividend growth rate and TFP are from CRSP and Compustat. The sample period for returns and dividend growth rates is from 1926 to December 2021. For TFP, the sample is from 1964 to 2020 at an annual frequency. For the model moments in Panel B, we compute averages and standard deviations across 500 simulations, each with a length of 100 years. Each moment from the model is constructed akin to its data counterpart.

	Growth (1)	(2)	(3)	(4)	(5)	(6)	(7)	(8)	(9)	Value (10)	Spread (11)
Panel A: Data											
Returns											
Avg.	7.76	8.88	8.77	8.04	8.91	9.67	8.59	11.17	12.78	12.88	5.11
Std.	19.66	18.36	18.64	20.43	19.46	20.89	22.14	23.41	26.47	31.61	22.03
t-stat.	3.86	4.72	4.59	3.84	4.47	4.52	3.79	4.66	4.71	3.98	2.27
Dividend Growth											
Avg.	4.07	6.48	4.05	4.55	5.53	5.00	5.72	8.41	13.24	13.51	9.44
Std.	26.73	29.71	22.53	29.67	26.94	26.57	30.37	33.89	42.06	50.65	60.28
t-stat.	1.47	2.10	1.73	1.48	1.98	1.81	1.82	2.39	3.04	2.57	1.51
TFP											
Avg.	0.79	1.33	0.58	0.69	0.54	−0.32	−0.60	−0.81	−1.10	−1.52	−2.32
Std.	1.80	1.62	1.41	1.41	1.83	1.56	1.89	2.06	1.85	2.38	3.06
t-stat.	3.32	6.21	3.10	3.70	2.21	−1.57	−2.40	−2.95	−4.48	−4.83	−5.72
Panel B: Model											
Returns											
Avg.	8.73	9.45	9.88	10.19	10.49	10.83	11.16	11.55	12.02	12.88	4.15
Std.	14.70	15.62	16.22	16.70	17.22	17.76	18.40	19.22	20.39	23.20	10.63
t-stat.	5.56	5.85	6.11	6.20	6.25	6.43	6.37	6.26	5.88	4.87	2.57
Dividend Growth											
Avg.	0.18	1.89	3.17	4.46	5.69	6.97	8.30	9.69	11.12	11.72	11.55
Std.	22.01	23.90	25.24	26.51	27.64	28.73	29.74	30.62	31.22	30.02	37.25
t-stat.	0.08	0.79	1.26	1.69	2.06	2.43	2.80	3.17	3.57	3.92	3.11
TFP											
Avg.	1.22	0.76	0.51	0.30	0.12	−0.06	−0.26	−0.47	−0.75	−1.30	−2.52
Std.	0.46	0.30	0.21	0.14	0.09	0.08	0.12	0.19	0.29	0.49	0.95
t-stat.	7.24	7.05	6.99	6.53	5.10	−4.91	−6.99	−7.07	−7.12	−7.20	−7.27

where $\lambda_t = [\lambda_{xt} \quad \lambda_w]'$ is a 2x1 vector containing the conditional market prices of risk and $\beta_{jt} = [\beta_{jxt} \quad \beta_{jwt}]'$ is the corresponding 2x1 vector of conditional return betas. The market prices of long-run consumption risks vary only because of fluctuating macro uncertainty, while the market price of macro uncertainty risks is constant. Time-varying cross-sectional dispersion in the return betas is driven by fluctuating micro uncertainty, primarily operating through conditional cash flow exposures to long-run risks. We provide strong empirical support for the dependence of cash flow risk to micro uncertainty in Section 4.3.2. In short, the time series dynamics of cross-sectional risk premia depend on both micro and macro uncertainty fluctuations.

In contrast, we can show that the conditional aggregate equity premium depends only on macro uncertainty through the market price of risk:

$$E_t[r_{mt+1} - r_{ft}] = \beta_m' \lambda_t \tag{22}$$

Note that these approximate relations are only used to highlight intuition, as our model results are computed using the nonlinear numerical solution method (details in Appendix C). As documented in Section 2, we find a strong positive correlation between macro uncertainty and the equity premium at low frequencies according to the evidence from Lettau et al. (2007) and in line with the model predictions.

As risk premia primarily reflect compensation for long-run risks in our model, the time series dynamics of risk premia mainly reflect movements in the conditional market prices of risk and betas with respect to long-run risks. We, therefore, focus the ensuing discussion on compensation for long-run risks. Appendix B shows that the market price of long-run risks is increasing with respect to macro uncertainty, and the spread in conditional betas for small minus big and value minus growth are increasing with respect to micro uncertainty. We find that the effects of micro uncertainty on the conditional betas dominate the impact of macro uncertainty on the conditional market price of risk. As such, micro uncertainty drives the size and value premia dynamics at low frequencies. The equity premium

Table 7
Size and Value Premia Conditional on Micro Uncertainty: Data and Model.
This table reports average future returns, future dividend growth rates, and TFP spread prior to portfolio formations. Columns 1, 2, 3, and 4 refer to moments from the data (same as those reported in Table 1), while Columns 5, 6, 7, 8, and 9 refer to their counterparts in the model. For the data, Panel A reports the average future returns of size and value strategies over 10 subsequent years in high and low micro uncertainty periods. The details on the construction of micro uncertainty are in Section 2.2. We define high (low) micro uncertainty periods as years in which micro uncertainty is in the top (bottom) quartile of its distribution. The size strategy is a zero-cost portfolio long on the bottom decile based on market capitalization and short on the top decile. The value strategy is a zero-cost portfolio long on the highest decile based on book-to-market and short on the bottom decile. In Panels B and C, we compute the average dividend growth rates and the average spread in TFP between the extreme portfolio deciles. TFP is computed as the average TFP innovation over the 10-year window up to the portfolio formation date. Return and dividend growth spread are 10-year forward rolling window averages. The return data is from Ken French's website, while the dividend growth rate and TFP are from Compustat. The sample is from 1964 to 2020 at an annual frequency. We report annualized averages and Newey-West corrected t-statistics. For the model moments, we compute averages and standard deviations across 500 simulations, each with a length of 100 years. Each moment from the model is constructed akin to its data counterpart.

	Data				Model			
	Size		Value		Size		Value	
	Low σ_{zt} (1)	High σ_{zt} (2)	Low σ_{zt} (3)	High σ_{zt} (4)	Low σ_{zt} (5)	High σ_{zt} (6)	Low σ_{zt} (7)	High σ_{zt} (8)
Panel A: Returns Spread								
Avg.	-0.28	7.54	4.5	7.92	3.61	5.95	2.92	5.33
t-stat.	-0.15	5.6	1.82	3.27	1.3	2.03	1.15	2.21
Panel B: Dividend growth spread								
Avg.	6.17	8.49	4.98	7.02	13.43	12.6	11.95	11.28
t-stat.	3.53	8.59	2.91	4.62	7.89	7.93	8.5	8.32
Panel C: Average spread in TFP shocks								
Avg.	−2.65	−2.96	−2.12	−2.72	−1.88	−4.04	−1.49	−3.56
t-stat.	−6.81	−6.29	−8.23	−3.8	−4.43	−8.25	−3.97	−8.47

in the model only varies with macro uncertainty. The comovement in the expected excess returns to size, value, and market strategies is consequently determined by the joint dynamics of micro and macro uncertainty.

The first row of Table 7 reports summary statistics for the expected returns to size and value spread portfolios conditional on low and high micro uncertainty periods across 500 simulations, each with a length of 100 years. Persistent low (high) micro uncertainty regimes are defined as periods in which the value of micro uncertainty is below (above) the median value. Both value and size premia are increasing with respect to micro uncertainty.

Persistent micro uncertainty affects the conditional size and value premia in our model by generating time-varying dispersion in conditional betas, primarily operating through the cash flow exposures to long-run risks. Higher micro uncertainty increases the magnitude of firm-specific productivity innovations. Firms with characteristics that are positively correlated with low total factor productivity (Z), such as small and value firms, experience an even lower realization of Z at portfolio formation when micro uncertainty is higher. Due to mean reversion, the expected growth rate of Z is even higher for such firms given that their level of Z is further below the mean relative to when micro uncertainty is lower. As a consequence, small and value firms, which already have a high average productivity exposure to long-run risks (highlighted in Eq. (20)), find that their cash flows become even more exposed to long-run consumption risks when micro uncertainty increases. Conversely, when micro uncertainty is higher, firms with characteristics that are correlated with high Z, such as big and growth firms, experience an even higher realization of Z at portfolio formation, but expect even lower growth, further reducing exposure to long-run risks. Overall, the model predicts higher micro uncertainty magnifies dispersion in TFP, and expected dividend growth across the size and book-to-market dimensions. The remaining rows of Table 7 provide empirical support for these conditional model dynamics. The difference in TFP and expected dividend growth between small and big decile portfolios (left panel) and between value and growth decile portfolios (right panel) are both increasing in absolute magnitude and statistical significance with respect to micro uncertainty, in line with model simulations.

The model can quantitatively reproduce the instability of the size and value factors in short samples due to persistent micro uncertainty. We illustrate this point in two ways. The first way is showing that the model can reproduce the empirical observation that size and value premia are statistically insignificant (at the 5% level) when micro uncertainty is low, but significant when micro uncertainty is high (Table 7). The t-stat is 1.3 for the size premium and 1.15 for the value premia in the model when micro uncertainty is low, but the t-stats are greater than 2 when micro uncertainty is high for both. The fragility in the size and value factors tends to arise in low micro uncertainty states because of the compression in the distribution in the conditional cash flow betas across the size and B/M dimensions. Section 4.3.2 provides evidence supporting the cash flow beta effect and Section 4.5 describes how the model frictions affect the fragility results.

Table 8
Fragility of Size and Value Premia.
This table illustrates how persistent micro uncertainty contributes to instability in size and value premia in short samples from the model. We report the fraction of simulations with an insignificant size premium (Columns 1, 2, 3, and 4) and value premium (Columns 5, 6, 7, and 8) for sample sizes of 20, 30, 40, and 50 years across 500 simulations at the 10%, 5%, and 1% significance levels. Panel A reports these statistics for the benchmark specification. Panel B does the same for a specification where we make micro uncertainty constant by setting $\zeta_z = 0$ while keeping the rest of the parameters the same as the benchmark.

	Percentage of simulations with insignificant size premium				Percentage of simulations with insignificant value premium			
	(1)	(2)	(3)	(4)	(5)	(6)	(7)	(8)
Panel A: Benchmark Calibration								
Sample Length (years)	20	30	40	50	20	30	40	50
Simulations with $p > 0.10$	29.4	18.6	12.0	9.0	28.2	19.6	12.2	9.4
Simulations with $p > 0.05$	42.2	27.0	18.8	12.6	42.0	27.8	18.6	13.2
Simulations with $p > .01$	65.2	50.2	38.4	28.8	66.2	51.4	39.2	29.8
Panel B: $\zeta_z = 0$								
Sample Length (years)	20	30	40	50	20	30	40	50
Simulations with $p > 0.10$	17.8	7.8	4.6	3.0	16.2	7.0	4.6	2.8
Simulations with $p > 0.05$	24.6	13.8	7.8	4.4	25.2	12.4	7.6	4.8
Simulations with $p > 0.01$	51.4	32.0	18.0	9.8	51.2	29.4	17.2	9.8

The second way we characterize how persistent micro uncertainty contributes to fragility in short samples of different lengths is presented in Table 8. This table reports the fraction of simulations that have an insignificant size premium and value premium for sample sizes of 20, 30, 40, and 50 years across 500 simulations and at the 10%, 5%, and 1% significance levels. We show these fragility statistics in the benchmark calibration (Panel A) and an alternative specification of the benchmark model with constant micro uncertainty by setting $\zeta_z = 0$ (Panel B). This table shows that the fraction of insignificant size and value premia across the independent simulations are significantly higher in the benchmark model that features fluctuating micro uncertainty, especially in shorter samples. For example, in simulations with a length of 20 years, the fraction of insignificant size and value premia in the benchmark model is almost twice as high as in the model with constant micro uncertainty.

4.3.1. Dynamic responses

This section quantitatively evaluates the dynamic responses of the size, value, and market premia to a common uncertainty shock, both in the model and data, by computing impulse response functions using local projections following Jordà (2005). These responses provide further empirical support for the model mechanics generating the comovement patterns between risk premia and uncertainty. Common negative variation between micro and macro uncertainty at low frequencies is captured by the common uncertainty component (ν_t) specified in Eq. (9). The impact of ν_t on macro and micro uncertainty is given by Eqs. (8) and (14), respectively. The process ν_t drives the dynamics of aggregate and cross-sectional risk premia through the market prices of risk and conditional betas.

As described in Section 4.1.1, the common uncertainty component is measured in the data by computing the first principal component ($PC1$) of the low-frequency micro and macro series. Let h index years ranging from 1 to 10. We run linear projections of the low-frequency component of size, value, and market premia on the common component, $PC1_t$:

$$RP_{s,t+h} = \alpha_{s,h} + \beta_{s,h} PC1_t + \xi_{s,t+h}, \tag{23}$$

where $RP_{s,t+h}$ is the low-frequency component of risk premium s in year $t+h$, and j indexes for the market, size and value premia, $\alpha_{s,h}, \beta_{s,h}$ are the projection coefficients, and $\xi_{s,h,t}$ is the projection residual. The impulse response function of $RP_{s,t}$ with respect to $PC1_t$ is given by the coefficients, β_h. We compute the impulse response functions using this local projection approach in the model and the data.

Fig. 5 plots the impulse response functions of the low-frequency component of the market, size, and value premia to a positive one standard deviation common uncertainty shock in the data (Panel A) and the model (Panel B). The shaded blue area corresponds to the 95% confidence bands from the data computed using Newey and West (1987) standard errors. Recall that the calibration of the uncertainty processes implies that a positive common uncertainty shock increases micro uncertainty but decreases macro uncertainty, which captures the negative long-run comovement between the two uncertainty series. Higher micro uncertainty increases the dispersion in conditional betas, while lower macro uncertainty reduces the market price of risk. The size premium and value premium increase in response to the positive common uncertainty shock, suggesting that the increase in the dispersion of the conditional betas across the size and *B/M* dimensions dominates the fall in the market price of risk. The conditional equity premium falls with the decline in the market price of risk.

4.3.2. Cash flow betas

This section quantitatively examines how the cash flow exposures to long-run risks across the size and *B/M* dimensions are impacted by micro uncertainty. The cash flow betas are the main channel for which persistent micro uncertainty impacts the dynamics of the size and value premia in the model. We find strong empirical support for

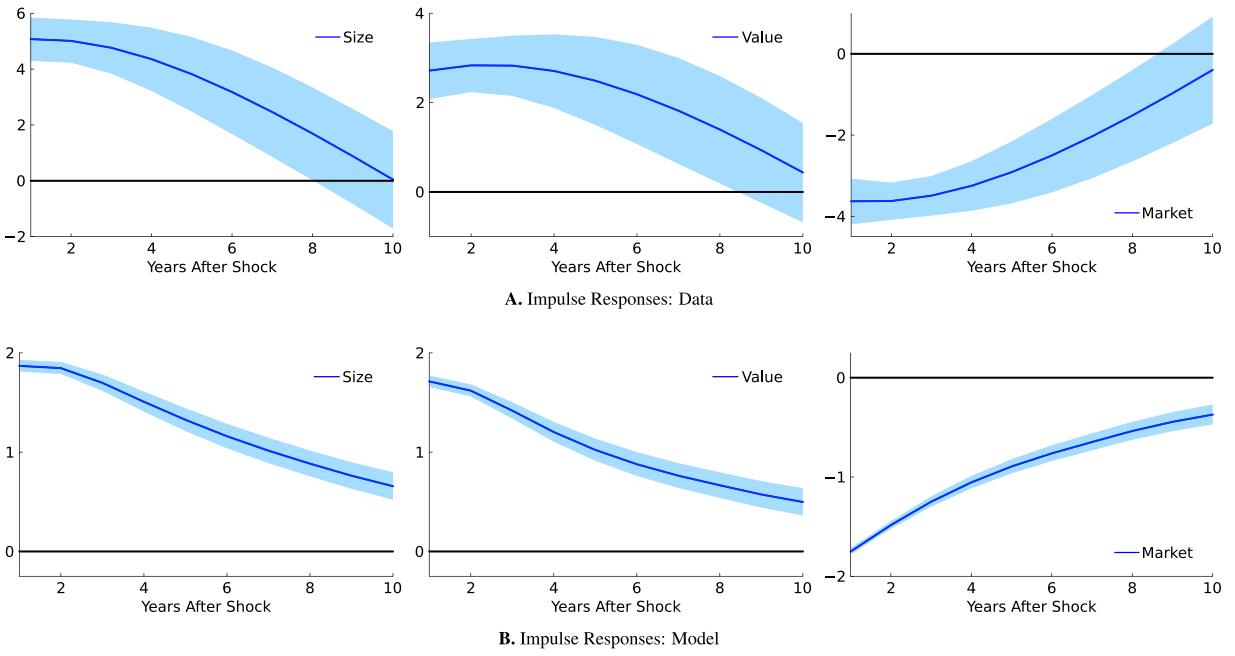

Fig. 5. Impulse response functions.
This figure plots impulse response functions (IRF) of the low-frequency market, size, and value premia to a one standard deviation shock to the common low-frequency component, which affects micro uncertainty positively and macro uncertainty negatively. Panel A refers to moments from the data, while Panel B refers to their counterparts in the model. The IRF are computed using local projections following Jordà (2005). First, we compute the first principal component of micro and macro uncertainty low-frequency series ($PC1_t$). Second, we run several regressions of our low-frequency risk premium variables (market, size, or value) on $PC1_{t-h}$, where we vary h from 1 to 10 years. Finally, in each panel below, we plot the estimated slope and its 95 percent confidence interval against h using asymptotic Newey and West (1987) robust standard errors (with ten lags). The details on the construction of micro and macro uncertainty are in Sections 2.2 and 2.3, and we obtain the low-frequency components of both micro and macro uncertainty by applying the Christiano and Fitzgerald (2003) band-pass filter to isolate frequencies between 25 and 50 years. The common component in the Jorda regressions is the first principal component of the low-frequency micro and macro uncertainty measures. For market risk premium, we compute a 10-year forward rolling window average excess return from year $t+1$ to year $t+10$. Similarly, for size and value, we compute a 10-year forward rolling window average from year $t+1$ to year $t+10$ of zero-cost small-minus-big and value-minus-growth portfolios. We obtain the low-frequency components of market, size, and value premia series by applying the band-pass filter to isolate frequencies between 25 and 50 years. All return series are average percent per year, and the impulse response functions measure the response of the size (left panel), value (middle panel), and market (right panel) premia to a one standard deviation shock to the common component of micro and macro uncertainty measures. For the model impulse response, we run the Jorda regressions akin to the data across in 500 simulations, each with a length of 100 years. In Panel B, we report the average response function across all the simulations.

the positive link between the dispersion in cash flow betas with respect to micro uncertainty.

We define the cash flow beta as the covariance between payout growth and the stochastic discount factor:

$$\beta_{it}^{CF} \equiv \frac{\text{Cov}_t(M_{t+1}, \Delta D_{it+1})}{\text{Var}_t(M_{t+1})},$$

where $\Delta D_{it+1} \equiv D_{it+1}/D_{it}$ is payout growth and M_{t+1} is the stochastic discount factor.[5]

Using a simple model with a similar shock structure, but assuming that firms have the same fixed capital stock only for illustrative purposes, we can show using approximate analytical solutions that the cash flow beta only depends on the covariance of payout growth with long-run risks. Appendix B provides the derivations of the simple model. Assuming that the cash flow betas are positive for expositional ease in the example below, we can write the log cash flow beta in the simple model as:

$$\log(\beta_{it}^{CF}) = -(1-\rho_z)\log(Z_{it}) + \frac{1}{2}\sigma_{zt}^2 + \log\left(\overline{\beta}_t^{CF}\right), \quad (24)$$

where the cash flow beta of the aggregate dividend claim, $\overline{\beta}_t^{CF}$, is a function of the state variables x_t and σ_t^2. The dispersion in cash flow betas across two firms i and j is then:

$$\log(\beta_{it}^{CF}) - \log(\beta_{jt}^{CF}) = -(1-\rho_z)[\rho_z(\log(Z_{it-1}) - \log(Z_{jt-1})) + \sigma_{zt-1}(\varepsilon_{it} - \varepsilon_{jt})] \quad (25)$$

where we used $\log(Z_{it}) = \rho_z \log(Z_{it-1}) + \sigma_{zt-1}\varepsilon_{it}$. Recall that small cap and value firms have low Z while big cap and growth firms have high Z. Suppose that we sort a large number of firms into deciles in our simple model based on Z and that firm i is in the lowest Z decile while firm j is in the highest Z decile. On average, the portfolio sorts would imply that $Z_{it-1} < Z_{jt-1}$ and $\varepsilon_{it} < \varepsilon_{jt}$, which generates a positive spread in cash flow betas since $0 \leq \rho_z < 1$. A persistent micro uncertainty process implies that the distribution of Z converges approximately to $\mathcal{N}(0, \sigma_{zt-1}^2/(1-$

[5] The cash flow beta relates to the return beta β_{it}^M in a no-arbitrage setting ($E_t[R_{it+1}] = R_{ft} + \beta_{it}^M \lambda_t^M$) according to: $\beta_{it}^M = \frac{D_{it}}{P_{it}}\left(\beta_{it}^{CF} + \beta_{it}^{VR}\right)$, where P_{it} is the *ex*-dividend price and $\beta_{it}^{VR} \equiv \text{Cov}_t(M_{t+1}, P_{it+1}/D_{it})/\text{Var}_t(M_{t+1})$.

Table 9
Cash flow betas.
This table evaluates the cash flow risk channel for explaining the size and value premia in the data (Panel A) and the model (Panel B). We measure cash flow betas in two steps. We first regress quarterly consumption growth on a one-year moving average of past consumption growth. The fitted values of this regression are a proxy for long-run consumption risks. The second step runs four-year rolling window regressions of four-year future payout growth on the measure of long-run risks for each of the 20 size and *B/M* decile portfolios i to obtain the quarterly time series of cash flow betas $\hat{\beta}_{it}^{CF}$. The column labeled 'Unconditional Regression' runs a cross-sectional regression of average returns on average cash flow betas across the 20 portfolios: $(1/T)\sum_t R_{it} = \lambda_0 + \lambda_1 (1/T)\sum_t \hat{\beta}_{it}^{CF} + w_i$. We report the slope coefficient λ_1 from this regression along with the corresponding t-statistic computed using Newey-West standard errors and the R^2 in the data (Panel A). The regression statistics from the model are averages across 500 simulations of 100 years (Panel B). The columns labeled 'Regressions Conditional on Micro Uncertainty' examines how differences in cash flow betas within a characteristic depend on micro uncertainty. For a given characteristic $j \in \{\text{size}, B/M\}$ at time t, we run a time-series regression of the difference in cash flow betas between decile 1 and decile 10 for a given characteristic j (BS_{jt}) on our estimated micro uncertainty series $\hat{\sigma}_{zt-1}$: $BS_{jt} = b_{j0} + b_{j1}\hat{\sigma}_{zt-1} + \omega_{jt}$. The estimated micro uncertainty series, $\hat{\sigma}_{zt-1}$, is computed following the steps outlined in Section 2.2 in the data and model simulations. We report the slope coefficients (b_{j1}) from this regression along with the corresponding t-statistic computed using Newey-West standard errors and the R^2 in the data (Panel A) and averages across model simulations (Panel B). We report these regressions separately for the size and *B/M* portfolios under the columns labeled 'Size Premium' and 'Value Premium,' respectively.

	Unconditional Regression	Regressions Conditional on Micro Uncertainty	
		Size Premium	Value Premium
Panel A: Data			
Slope Coeff.	0.64	−1.04	0.65
t-stat.	2.86	−2.86	1.85
R^2	0.31	0.06	0.15
Panel B: Model			
Slope Coeff.	0.79	−0.42	0.68
t-stat.	3.00	−2.39	4.00
R^2	0.38	0.07	0.08

$\rho_z^2)$). Hence, both components of Eq. (25), $(\log(Z_{it-1}) - \log(Z_{jt-1}))$ and $\sigma_{zt-1}(\varepsilon_{it} - \varepsilon_{jt})$, increase with respect to micro uncertainty (σ_{zt-1}), implying that the dispersion in cash flow betas is positively related to micro uncertainty. We test these predictions next.

Table 9 provides evidence for the cash flow exposures to long-run risks across the 20 size and book-to-market decile portfolios. The construction of cash flow betas measuring exposures to long-run risks are estimated in a similar way as Bansal et al. (2005). First, quarterly consumption growth is regressed on a K-period moving average of past consumption growth:

$$\Delta c_t = a_0 + a_1 \left(\frac{1}{K} \sum_{k=1}^{K} \Delta c_{t-k} \right) + u_{it}, \tag{26}$$

where a_0 and a_1 are the regression coefficients and u_{it} is the residual. We use $K = 4$ quarters for computing the moving average in our benchmark specification. The fitted values from the regression, $\Delta\hat{c}_t = \hat{a}_0 + \hat{a}_1\left(\frac{1}{K}\sum_{k=1}^{K}\Delta c_{t-k}\right)$, provide a measure of long-run consumption risks. Second, conditional cash flow betas for each portfolio i are obtained by estimating a rolling regression of the five-year future payout growth on the estimated measure of long-run risks from the first step:

$$\Delta d_{it\to t+5} = \alpha_i + \hat{\beta}_{it}^{CF} \cdot \Delta\hat{c}_t + \nu_{it}, \tag{27}$$

over a four-year rolling window. These regressions yield a time series of quarterly cash flow betas ($\hat{\beta}_{it}^{CF}$) that measure conditional cash flow exposures to long-run risks.

Before analyzing the patterns in betas conditional on micro uncertainty, we begin by confirming that unconditional differences in the estimated cash flow betas can account for average returns across the size and *B/M* decile portfolios, inline with the unconditional model predictions outlined in Section 4.2. Returns and cash flow betas are averaged over time t within each portfolio i and we run the following cross-sectional regression across the 20 portfolios:

$$\frac{1}{T}\sum_t R_{it} = \lambda_0 + \lambda_1 \frac{1}{T}\sum_t \hat{\beta}_{it}^{CF} + w_i. \tag{28}$$

Column 1 of Table 9 reports the cross-sectional regression results in the data (Panel A) and the model (Panel B), where we use the same empirical procedure. The model estimates are the averages across 500 simulations of 100 years each. The cash flow betas explain over a quarter of the variation in expected returns across the 20 portfolios. The slope coefficient related to the market price of long-run risks is positive and statistically significant, consistent with the empirical findings from Bansal et al. (2005).

Our model predicts that when micro uncertainty rises, the absolute difference in the cash flow exposure of long-run risks across size and book-to-market portfolios increases, as illustrated in equation (25). We assess the con-

ditional relation between the difference in cash flow betas across the extreme decile portfolios and the persistent component of micro uncertainty by running the following time-series regression for each characteristic $j \in \{\text{size}, B/M\}$:

$$BS_{jt} = b_{j0} + b_{j1}\hat{\sigma}_{zt-1} + \omega_{jt}, \tag{29}$$

where BS_{jt} is the spread in cash flow betas between the decile 1 portfolio and decile 10 portfolio of characteristic j and $\hat{\sigma}_{zt-1}$ is the estimate of micro uncertainty calculated using the procedure outlined in Section 2.2. Columns 2 and 3 of Table 9 report the time-series regression results on the conditional relation for size and value premium, respectively. Both in the data (Panel A) and the model (Panel B), we find that the absolute difference in the cash flow betas increases with micro uncertainty within each characteristic consistent with model predictions. The negative relation between size and cash flow betas becomes more negative, while the positive relation between book-to-market and cash flow betas becomes more positive with higher micro uncertainty. This evidence also highlights how the compression in cash flow betas across decile portfolios for a given characteristic is a source of instability in size and value premia in small samples when micro uncertainty is low.

4.4. Comovement

This section demonstrates that the model can explain the comovement patterns in uncertainty and risk premia at low frequencies documented in Section 2.4. The persistent common factor in micro and macro uncertainty (ν_t) drives the low-frequency patterns in risk premia in the model through distinct channels. The impact of ν_t on macro uncertainty operates through the market price of risk, while the impact of ν_t on micro uncertainty affects the dispersion in conditional cash flow betas. We assume the common factor impacts micro and macro uncertainty in opposite directions to explain the strong negative correlation between micro and macro uncertainty illustrated in Fig. 3. Clara et al. (2021) can endogenously explain the negative relation between micro and macro uncertainty in a general equilibrium model featuring oligopolistic firms that endogenously choose product scope. They find that rising barriers to entry lead incumbent firms to consolidate market power by diversifying production, leading to lower micro uncertainty. The increase in industry concentration also makes incumbent firms more susceptible to aggregate entry risk, implying higher macro uncertainty.

Table 10 reports the pairwise correlations between the size premium, value premium, equity premium, micro uncertainty, and macro uncertainty at low frequencies in the data and the model. The model correlations are population moments. We obtain the low-frequency components of each series using the bandpass filter discussed in Section 2.1. The model can reproduce the strong positive comovement between the size premium, value premium, and micro uncertainty, while simultaneously explaining the strong negative comovement between the equity premium with both the size and value premium.

The common uncertainty factor (ν_t) drives the low-frequency risk premia dynamics in the model. A negative shock to ν_t increases micro uncertainty and decreases macro uncertainty. Higher micro uncertainty increases dispersion in cash flow betas across the size and book-to-market dimensions, raising size and value premia, all else equal. However, higher micro uncertainty is associated with lower macro uncertainty, which reduces the market price of long-run risks, leading to the opposite effect on size and value risk premia. We find that the effects of micro uncertainty on size and value premia dynamics dominate, leading to the strong positive comovement. The conditional equity premium only depends on macro uncertainty in a positive way through the market price of risk. As macro uncertainty is negatively correlated with micro uncertainty, size and value premia are both negatively related to the equity premium. These strong correlations at low frequencies also suggest that the market factor is a good hedge for value and size strategies for a long-term investor.

4.5. Inspecting the mechanism

This section investigates the role of the uncertainty processes and investment frictions in generating the main asset pricing results. To this end, Table 11 compares key moments for alternative model specifications with the benchmark calibration. Column (1) is the benchmark calibration. Column (2) assumes constant macro uncertainty by setting $\varsigma = 0$. Column (3) examines the case of constant micro uncertainty by calibrating $\varsigma_z = 0$. Column (4) assumes symmetric quadratic adjustment costs ($\theta^+ = \theta^- = 315$). Column (5) uses both symmetric quadratic adjustment costs ($\theta^+ = \theta^- = 315$) and shuts down the proportional fixed costs ($f = 0$). In each of these alternative model specifications, we keep the rest of the parameter values the same as the benchmark.

With either constant macro uncertainty ($\varsigma = 0$) or constant micro uncertainty ($\varsigma_z = 0$), the unconditional size and value premia increase relative to the benchmark specification. The negative correlation between micro and macro uncertainty in the benchmark creates a hedging effect between the dispersion in conditional betas and the market price of risk that reduces risk premia, which we can see in the approximate expected return-beta representation outlined in Eq. 21. The higher size and value premia in these two alternative specifications are also reflected in the larger slope coefficient from the cross-sectional regression of expected returns on cash flow betas described in Section 4.3.2. Constant macro uncertainty implies that the market prices of risk are constant while constant micro uncertainty implies that the distribution of betas across characteristics is constant. Either scenario eliminates the hedging effect present in the benchmark model, raising unconditional risk premia.

The constant macro uncertainty specification ($\varsigma = 0$) implies a constant market price of risk, which translates to a constant equity premium, illustrated in the approximate relation shown in Eq. 22. Consequently, the correlation between the equity premium with both size and value premia is close to zero with constant macro uncertainty.

Table 10
Low-frequency correlations.
This table reports low-frequency correlations between market risk, size and value risk premia, and micro and macro uncertainty. Columns 2, 3, 4, 5, and 6 refer to correlation from the data, while Columns 7, 8, 9, 10, and 11 refer to their counterparts in the model. For market risk premium, we compute a 10-year forward rolling window average excess return from year $t+1$ to year $t+10$. Similarly, for size and value, we compute a 10-year forward rolling window average from year $t+1$ to year $t+10$ of zero-cost small-minus-big and value-minus-growth portfolios. The details on the construction of micro and macro uncertainty are in Sections 2.2 and 2.3. To obtain the low-frequency components of these series, we apply the Christiano and Fitzgerald (2003) band-pass filter to isolate frequencies between 25 and 50 years. For the model correlation, we compute the low-frequency correlation in 500 simulations, each with a length of 100 years, and then we report the average low-frequency correlations across the simulations.

	Data					Model				
Variable (1)	Size (2)	Value (3)	Market (4)	Micro (5)	Macro (6)	Size (7)	Value (8)	Market (9)	Micro (10)	Macro (11)
Size	1.00	0.94	−0.99	0.92	−0.91	1.00	0.98	−0.49	0.58	−0.58
Value	–	1.00	−0.91	0.86	−0.77	–	1.00	−0.47	0.55	−0.55
Market	–	–	1.00	−0.95	0.88	–	–	1.00	−0.96	0.96
Micro	–	–	–	1.00	−0.77	–	–	–	1.00	−1.00
Macro	–	–	–	–	1.00	–	–	–	–	1.00

Table 11
Alternative model specifications.
This compares alternative specifications of the model with the benchmark specification. Panel A reports the average size, value, and market risk premia along with the slope coefficient from the cross-sectional regression of expected returns on the cash flow betas described in Section 4.3.2. Panel B presents the pairwise low-frequency correlations between size, value, and market risk premia. Panel C displays the t-stats of the size and value premia conditional on low and high micro uncertainty in short samples outlined in Section 4.3. Column (1) reports the results of the benchmark calibration. The remaining columns examine alternative specifications that shut down specific channels. Column (2) assumes constant macro uncertainty ($\varsigma = 0$). Column (3) considers constant micro uncertainty ($\varsigma_z = 0$). Column (4) uses symmetric quadratic adjustment costs ($\theta^+ = \theta^-$). Column (5) assumes symmetric adjustment costs ($\theta^+ = \theta^-$) and no proportional fixed costs ($f = 0$).

	benchmark (1)	$\varsigma = 0$ (2)	$\varsigma_z = 0$ (3)	$\theta^+ = \theta^-$ (4)	$\theta^+ = \theta^-$ $f = 0$ (5)
Panel A: Unconditional Risk Premia					
Equity Premium	9.98	10.29	11.50	8.76	7.86
Size Premium	4.76	6.05	7.09	2.66	1.17
Value Premium	4.15	5.28	6.49	2.61	0.85
Return-Cash flow beta slope	0.79	1.07	1.41	0.70	0.22
Panel B: Low-Frequency Correlations					
Corr(size,value)	0.98	0.99	0.99	0.99	0.85
Corr(equity,size)	−0.49	−0.03	0.62	−0.17	−0.50
Corr(equity,value)	−0.47	−0.01	0.57	−0.17	−0.75
Panel C: Fragility Statistics					
T-stat size premium (low micro uncertainty)	1.30	1.51	2.75	0.33	3.25
T-stat size premium (high micro uncertainty)	2.03	2.52	2.96	0.99	2.75
T-stat value premium (low micro uncertainty)	1.15	1.31	2.80	0.34	2.54
T-stat value premium (high micro uncertainty)	2.21	2.93	3.08	1.13	2.72

We still get a strong positive correlation between size and value at low frequencies in this specification because size and value premia dynamics are driven by micro uncertainty. The constant micro uncertainty specification ($\varsigma_z = 0$) implies a constant distribution of cash flow betas across characteristics. Consequently, the variation in aggregate and cross-sectional risk premia are driven by persistent macro uncertainty through the market price of risk when $\varsigma_z = 0$, leading to strong positive comovement between size, value, and equity premia. The benchmark specification is able to explain the negative comovement between the equity premium with both size and value premia through the negative relation between micro and macro uncertainty at low frequencies. The impact of persistent micro uncertainty on the dispersion in conditional betas dominates the opposing effect of persistent macro uncertainty on the market price of risk in the benchmark specification, allowing size and value premia to increase with micro uncertainty. As the equity premium increases with macro uncertainty, the opposing micro-macro uncertainty dynamics produce the negative low-frequency movements between aggregate and cross-sectional risk premia observed in the data.

Persistent micro uncertainty is critical for generating fragility in size and value premia in short samples. Low micro uncertainty periods compress the distribution of conditional betas, weakening the statistical significance. Shutting down micro uncertainty ($\varsigma_z = 0$) generates greater stability

in the size and value factors. In particular, we showed previously in Table 8 how shutting down micro uncertainty reduced the percentage of insignificant short sample simulations. The specification with constant macro uncertainty ($\varsigma = 0$) in Table 11 shows that the fragility results are not driven by the effects of persistent macro uncertainty and its negative correlation with micro uncertainty. We show that the insignificance of size and value conditional on low micro uncertainty and the significance conditional on high micro uncertainty is preserved with constant macro uncertainty.

The final two columns of Table 11 characterize the role of key investment frictions. The specification with symmetric quadratic adjustment costs ($\theta^+ = \theta^-$) decreases risk premia relative to the benchmark, which assumes that disinvestment is costlier than investment ($\theta^- > \theta^+$). The asymmetry in adjustment costs makes it more difficult for low-productivity firms (i.e., small and value firms) to disinvest in bad times, exposing the cash flow of these firms more to long-run risks, contributing to a larger size and value premia in the benchmark. This is also reflected in a larger slope from the cross-sectional regression of expected returns on the cash flow betas across the size and B/M portfolios. Shutting down the fixed costs proportional to the capital stock ($f = 0$) on top of the specification with symmetric adjustment costs further reduces risk premia but has a larger impact on the value premium. The value premium is only 2% smaller than the size premium in the case with only symmetric adjustment costs ($\theta^+ = \theta^-$), while it is 40% smaller in the specification with symmetric adjustment costs and fixed proportional costs ($\theta^+ = \theta^-$ and $f = 0$). The reason why the proportional fixed costs are more critical for the value premium is that value firms have large capital stocks, making the operating leverage from the proportional component, fK_{it}, larger compared to small cap firms that are characterized by small capital stocks.

The investment frictions also contribute to the insignificance of size and value premia in low micro uncertainty states but significance in high micro uncertainty states. With symmetric quadratic adjustment costs ($\theta^+ = \theta^-$), size and value premia are insignificant across high and low micro uncertainty periods. Symmetric adjustment costs reduce the cash flow exposure to bad aggregate states compared to the benchmark specification, lowering risk premia. However, given that the average level of adjustment costs stays about the same, the volatility of returns is less affected, contributing to the insignificant size and value premia in both low and high micro uncertainty states. Setting proportional fixed costs to zero on top of symmetric adjustment costs ($\theta^+ = \theta^-$ and $f = 0$) makes size and value significant in both low and high micro uncertainty states. Eliminating operating leverage from the proportional component reduces the volatility of size and value premia more than the means.

5. Conclusion

This paper documents how common variations in size and value premia are negatively related to movements in the equity premium at low frequencies. We show that incorporating a persistent common factor in micro and macro uncertainty in an investment-based asset pricing model can rationalize these low-frequency patterns. This common factor is assumed to impact micro and macro uncertainty in opposite directions to explain their strong negative correlation at low frequencies. Persistent micro uncertainty generates time-varying dispersion in conditional betas across size and book-to-market sorts, while persistent macro uncertainty produces a time-varying market price of risk.

The negative relation between micro and macro uncertainty leads to opposing movements between the market price of risk and the dispersion in conditional betas across the characteristics sorts. Our calibrated model predicts that the dispersion in betas dominates the market price of risk, implying that size and value are both increasing with micro uncertainty. As the equity premium increases with macro uncertainty, the opposing movements in micro and macro uncertainty imply that the equity premium is a long-run hedge to both size and value premia.

Model simulations suggest that persistent micro uncertainty is a source of instability for the size and value factors. Our model can explain why we find an insignificant size and value premia when micro uncertainty is low but significant ones when micro uncertainty is high. Periods of low micro uncertainty compress the distribution of betas, reducing size and value premia and weakening their statistical significance in short samples. We find strong empirical support for the positive relationship between the dispersion in cash flow betas and micro uncertainty predicted by our model. Overall, our paper highlights the importance of persistent micro uncertainty for explaining asset price fluctuations.

Declaration of Competing Interest

I have nothing to declare.
Bernard Herskovic
I have nothing to declare.
Thilo Kind
I have nothing to declare.
Howard Kung

Data availability

Data will be made available on request.

Appendix A. Empirics

A1. Payout growth calculation

We use cum-dividend returns (RET) and ex-dividend returns (RETX) adjusted for splits to compute the implied dividend growth rate at the portfolio level. First we adjust ex-dividend returns (RETX) at month $t + 1$ by multiplying it by $\min\{n_{t+1}, n_t, 1\}$, where n_t is the product of the total number of shares outstanding (SHROUT) and the cumulative factor to adjust shares (CFACSHR). Let the cum-dividend value-weighted return of portfolio i from month

t to $t+1$ be given by

$$R_{i,t+1} = \frac{V_{i,t+1} + D_{i,t+1}}{V_{i,t}},$$

where $V_{i,t}$ is the total market value of the portfolio and $D_{i,t+1}$ includes all portfolio i's payouts. The adjusted ex-dividend return of the same portfolio is given by:

$$h_{i,t+1} = \frac{V_{i,t+1}}{V_{i,t}},$$

which is the value-weighted average of the ex-dividend return adjusted for splits.

Hence, we have

$$V_{i,t+1} = \prod_{\tau=0}^{t+1} h_{i,t+1} V_{i,0},$$

and

$$D_{i,t+1} = V_{i,t} \times (R_{i,t+1} - h_{i,t+1}) = V_{i,0} \left(\prod_{\tau=0}^{t} h_{i,t+1} \right) (R_{i,t+1} - h_{i,t+1}).$$

To compute the dividend growth rate of portfolio i, we compute $\frac{D_{i,t+1}}{V_{i,0}}$ using the formula above. Then, we define dividend growth rate as:

$$\text{DivGr}_{i,t+1} = \frac{D_{i,t+1}/V_{i,0}}{D_{i,t}/V_{i,0}} = \frac{D_{i,t+1}}{D_{i,t}}.$$

Finally, deflate dividend growth rates using FRED's consumer price index from FRED (variable CPIAUCSL).

A2. Robustness figures and tables

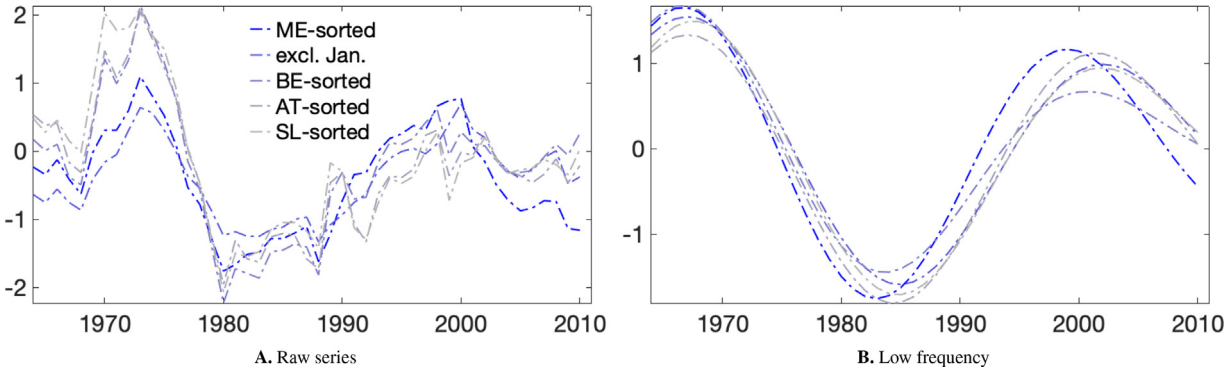

Fig. A.1. Robustness: Size premia with different size measures.
This figure shows the time series risk premium of different size-based strategies. We consider five different versions in which we sort stocks on the following measures for firm size: market capitalization (ME-sorted), market capitalization but excluding the month of January (excl. Jan.), book value of equity (BE-sorted), total assets (AT-sorted), total sales (SL-sorted). In all five versions, we report is a portfolio that goes long small (1^{st} decile) stocks and shor tbig stocks (10^{th} decile). We plot each series' 10-year forward rolling window average from year $t+1$ to year $t+10$ in the left panel. In the right panel, we plot the low-frequency components of these series, which are obtained after applying the Christiano and Fitzgerald (2003) bandpass filter to isolate frequencies between 25 and 50 years. To facilitate visual comparison, all series are standardized to have mean zero and variance one.

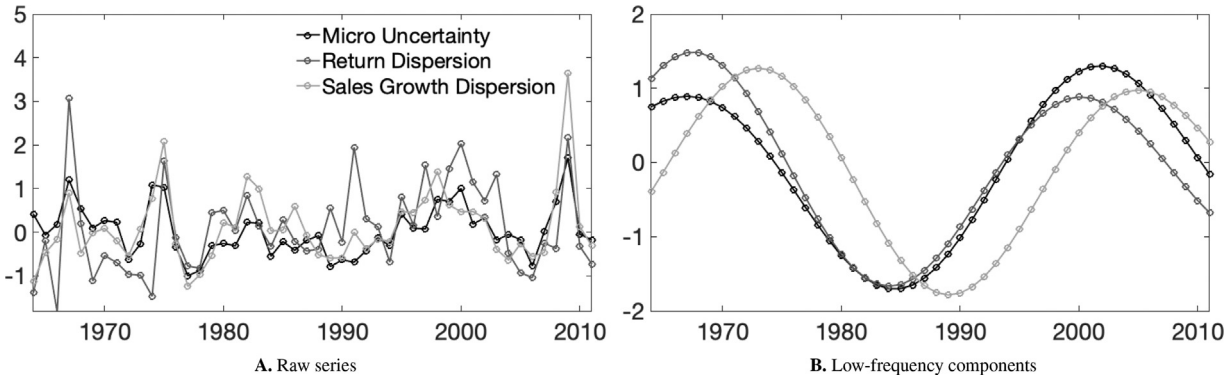

Fig. A.2. Alternative micro uncertainty measures.
This figure shows the time series comovement between the following measures of micro uncertainty: our benchmark micro uncertainty measure described in Section 2.2, cross-sectional dispersion in returns and cross-sectional dispersion in sales. To compute sales and return dispersion, we follow a similar methodology of our benchmark micro uncertainty series by reporting interquartile ranges. Specifically, return dispersion is the cross-sectional interquartile range of annual excess returns. For sales dispersion, we compute the detrended cross-sectional interquartile range of sales growth rates. In the left panel, we plot all three measures of micro uncertainty, and, in the right panel, we plot their low-frequency components, which are obtained after applying the Christiano and Fitzgerald (2003) bandpass filter to isolate frequencies between 25 and 50 years. To facilitate visual comparison, all series are standardized to have mean zero and variance one.

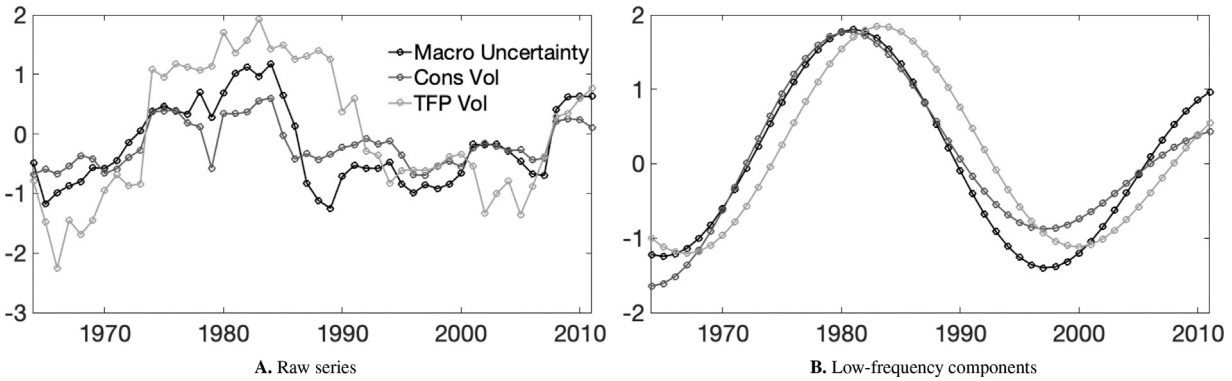

Fig. A.3. Alternative macro uncertainty measures.
This figure shows the time series comovement between the following measures of macro uncertainty: volatility of aggregate output growth (Macro Uncertainty), consumption growth (Cons Vol) and aggregate total factor productivity growth (TFP Vol). Volatility of output growth is our benchmark macro uncertainty measure described in Section 2.3. Consumption growth is the growth rate of real personal consumption expenditures, TFP growth is the growth of Total Factor Productivity at Constant National Prices for United States, and aggregate output growth is the growth rate of real gross domestic product for the United States. All three series are from the Federal Reserve Economic Data (FRED), and their respective volatilities are computed in a rolling window of 5 years from year $t-4$ to t. In the left panel, we plot the three volatility series, and, in the right panel, we plot the low-frequency components of these series, which are obtained after applying the Christiano and Fitzgerald (2003) bandpass filter to isolate frequencies between 25 and 50 years. To facilitate visual comparison, all series are standardized to have mean zero and variance one.

Table A.1
Robustness of comovement patterns.
This table reports correlations between market risk, size and value risk premia, and both micro and macro uncertainty. For market risk premium, we compute 10-year forward rolling window average excess return from year $t+1$ to year $t+10$. Similarly, for size and value, we compute 10-year forward rolling window average from year $t+1$ to year $t+10$ of zero-cost small-minus-big and value-minus-growth portfolios. The details on the construction of micro and macro uncertainty are provided in Sections 2.2 and 2.3. In the top panel, we report the correlations of the raw series between these five series. In the bottom panel, we report the correlation between these series' low-frequency components for different frequencies. To obtain the low-frequency components of these series, we apply the Christiano and Fitzgerald (2003) bandpass to filter for periods smaller than 8, 20 and 25, and larger than 50 and 75 years.

Panel A: Correlations (raw series)

	Size	Value	Market	Micro	Macro
Size	1.00	0.66	−0.55	0.32	−0.40
Value	–	1.00	−0.53	0.07	−0.07
Market	–	–	1.00	−0.27	0.33
Micro	–	–	–	1.00	−0.05
Macro	–	–	–	–	1.00

Panel B: Correlations (low-frequency)

	Maximum frequency of 50 years					Maximum frequency of 75 years				
Panel B.1: Minimum frequency of 8 years										
	Size	Value	Market	Micro	Macro	Size	Value	Market	Micro	Macro
Size	1.00	0.92	−0.65	0.57	−0.45	1.00	0.85	−0.57	0.54	−0.42
Value	–	1.00	−0.61	0.48	−0.29	–	1.00	−0.43	0.26	−0.15
Market	–	–	1.00	−0.68	0.57	–	–	1.00	−0.65	0.49
Micro	–	–	–	1.00	−0.18	–	–	–	1.00	−0.26
Macro	–	–	–	–	1.00	–	–	–	–	1.00
Panel B.2: Minimum frequency of 20 years										
	Size	Value	Market	Micro	Macro	Size	Value	Market	Micro	Macro
Size	1.00	0.94	−0.96	0.90	−0.79	1.00	0.82	−0.91	0.78	−0.78
Value	–	1.00	−0.83	0.79	−0.59	–	1.00	−0.63	0.36	−0.46
Market	–	–	1.00	−0.96	0.79	–	–	1.00	−0.80	0.69
Micro	–	–	–	1.00	−0.64	–	–	–	1.00	−0.62
Macro	–	–	–	–	1.00	–	–	–	–	1.00
Panel C.3: Minimum frequency of 25 years										
	Size	Value	Market	Micro	Macro	Size	Value	Market	Micro	Macro
Size	1.00	0.94	−0.99	0.92	−0.91	1.00	0.78	−0.94	0.83	−0.91
Value	–	1.00	−0.91	0.86	−0.77	–	1.00	−0.70	0.41	−0.66
Market	–	–	1.00	−0.95	0.88	–	–	1.00	−0.79	0.74
Micro	–	–	–	1.00	−0.77	–	–	–	1.00	−0.73
Macro	–	–	–	–	1.00	–	–	–	–	1.00

Appendix B. Simple Model

We use a simplified model to illustrate the key mechanisms of our quantitative benchmark specification. The simplified model abstracts from capital accumulation for analytical tractability. This model can be interpreted as a case where capital is fixed to a constant across time and firms. First, we solve for the price-dividend ratio of the aggregate dividend claim. Next, we compute the associated aggregate dividend strip prices. We introduce and price assets featuring maturity-dependent idiosyncratic weights on aggregate dividends. We show that this framework implies an approximate linear factor structure for expected returns. We provide closed-form solutions showing how the conditional cash flow betas vary across characteristics and depend on micro uncertainty.

B1. Representative household

Log consumption growth, Δc_{t+1}, features a persistent expected growth component, x_t, and time-varying stochastic volatility, σ_t^2, as in Bansal and Yaron (2004):

$$\begin{aligned}\Delta c_{t+1} &= \mu + x_t + \sigma_t \varepsilon_{ct+1},\\ x_{t+1} &= \rho_x x_t + \sigma_x \sigma_t \varepsilon_{xt+1},\\ \sigma^2_{t+1} &= \bar{\sigma}^2 + \nu\left(\sigma_t^2 - \bar{\sigma}^2\right) + \sigma_w w_{t+1}.\end{aligned}$$

As in Section 3.1, the representative agent has Epstein-Zin preferences such that the Euler equation and the corresponding stochastic discount factor reads

$$1 = E_t\left[\exp\left(\theta \log\beta - \frac{\theta}{\psi}\Delta c_{t+1} + (\theta-1) r_{ct+1} + r_{it+1}\right)\right],$$

$$m_{t,t+1} = \theta\log\beta - \frac{\theta}{\psi}\Delta c_{t+1} + (\theta-1) r_{ct+1},$$

where r_{ct+1} is the return on the consumption claim. The solution to the consumption claim is given by approximating the return using the Campbell-Shiller log-linearization and guessing a linear relation between the wealth to consumption ratio, wc_t, and the aggregate state variables, x_t and σ_t^2:

$$\begin{aligned}r_{ct+1} &= \kappa_{0c} + \kappa_{1c} wc_{t+1} - wc_t + \Delta c_{t+1},\\ wc_t &= A_0 + A_1 x_t + A_2 \sigma_t^2.\end{aligned}$$

Plugging the solution into the Euler equation and using the method of undetermined coefficients leads to the fixed point solution which has to be solved numerically.[6] The real riskfree rate is given by:

$$\begin{aligned}r_t^f &= -E_t[m_{t+1}] - \frac{1}{2}Var_t[m_{t+1}],\\ &= c_0 + c_1 x_t + c_2 \sigma_t^2.\end{aligned}$$

B2. Aggregate dividends

Following Section 3.2, aggregate dividends have a levered exposure to the long-run consumption growth risks component x_t:

$$\Delta d_{t+1} = \mu + \phi x_{t+1}.$$

The solution to the dividend claim also uses the method of undetermined coefficients:

$$\begin{aligned}r_{dt+1} &= \kappa_{0d} + \kappa_{1d} pd_{t+1} - pd_t + \Delta d_{t+1},\\ pd_t &= A_{d0} + A_{1d} x_t + A_{2d}\sigma_t^2.\end{aligned}$$

B3. Aggregate dividend strips

The log dividend strip prices scaled by current aggregate dividends are given by:

$$\begin{aligned}pd_t^n &= pd_t^1 + E_t\left[pd_{t+1}^{n-1}\right] + \frac{1}{2}Var_t\left[pd_{t+1}^{n-1}\right] + Cov_t\left(pd_{t+1}^{n-1}, m_{t+1}\right)\\ &\quad + Cov_t\left(pd_{t+1}^{n-1}, \Delta d_{t+1}\right)\\ pd_t^n &= C_{0n} + C_{1n} x_t + C_{2n}\sigma_t^2\end{aligned}$$

Thus, the beta representation of the expected return on a dividend strip is given by:

$$\begin{aligned}&E_t\left[r^n_{t,t+1} - r_{ft}\right] + \frac{1}{2}Var_t\left[r^n_{t,t+1}\right] =\\ &- Cov_t\left(m_{t+1}, pd_{t+1}^{n-1} - pd_t^n + \Delta d_{t+1}\right),\\ &= \lambda_{x,t}\beta^n_{m,x} + \lambda_w \beta^n_{m,w},\end{aligned}$$

with the beta definitions, $\beta^n_{m,x} \equiv -(C_{1n-1} + \phi)\sigma_x$ and $\beta^n_{m,w} \equiv -C_{2n-1}$.

B4. Cash flow beta

To analyze the cross-sectional implications, we consider a payout growth for firm i which follows aggregate dividend growth Δd_{t+1} in conjunction with an idiosyncratic multiplicative component:

$$\begin{aligned}D_{it+1} &= Z_{it+1} D_{t+1},\\ \log\left(Z_{it+1}\right) &= \rho_z \log\left(Z_{it}\right) + \sigma_{zt}\varepsilon_{it+1},\end{aligned}$$

where micro uncertainty σ_{zt} follows a stationary process. Then, the log cash flow beta for firm i reads:

$$\begin{aligned}\log\left(\beta_{it}^{CF}\right) &= -(1-\rho_z) z_{it} + \frac{1}{2}\sigma_{zt}^2 + \log\left(\frac{Cov_t\left(M_{t+1}, D_{t+1}/D_t\right)}{Var(M_{t+1})}\right)\\ &= -(1-\rho_z) z_{it} + \frac{1}{2}\sigma_{zt}^2 + \log\left(\overline{\beta}_t^{CF}\right).\end{aligned}$$

B5. Expected return and micro uncertainty

Consider a firm with firm-specific multiplicative dividend payouts, $Z^s_{it} \equiv E_t\left[Z^s_{it+s}\right] = E_t[D_{it+s}/D_{t+s}]$, i.e. the expected ratio between the firm dividend strip and the aggregate dividend strip which we assume is orthogonal to each other. Thus, the equity price of such a firm is given by:

$$P_{it} = E_t\left[\sum_{s=1}^{\infty} M_{t,t+s} D_{it+s}\right] = \sum_{s=1}^{\infty} Z^s_{it} P^s_t,$$

[6] The detailed solution to the coefficients A, B, and c are available upon request.

with the aggregate dividend strip price P_t^s. The corresponding return is:

$$R_{it+1} = \sum_s \underbrace{\frac{Z_{it}^s P_t^s}{P_{it}}}_{\equiv \Omega_{it}^s} \frac{Z_{it+1}^{s-1}}{Z_{it}^s} R_{t,t+1}^s,$$

where $R_{t,t+1}^s \equiv P_{t+1}^{s-1}/P_t^s$ is the strip return. Since $Z_{it}^s = E_t\left[Z_{it+1}^{s-1}\right]$, the expected return becomes:

$$E_t\left[\frac{R_{it+1}}{R_{ft}}\right] = \sum_s \Omega_{it}^s E_t\left[\frac{R_{t,t+1}^s}{R_{ft}}\right].$$

Using the beta expression for the expected dividend strip return and approximating around $\beta = 0$ leads to a log linear factor structure:

$$\begin{aligned} E_t\left[r_{it+1} - r_{ft}\right] &= \sum_s \Omega_{it}^s \left[\lambda_{x,t}\beta_{m,x}^s + \lambda_w \beta_{m,w}^s\right], \\ &= \lambda_{xt}\left(\sum_{s=1} \Omega_{it}^s \beta_{m,x}^s\right) + \lambda_w \left(\sum_{s=1} \Omega_{it}^s \beta_{m,w}^s\right), \\ &= \beta_{ixt}\lambda_{x,t} + \beta_{iwt}\lambda_w \end{aligned}$$

with weights $\sum_s \Omega_{it}^s = \sum_s \frac{Z_{it}^s P_t^s}{P_{it}} = \sum_s \frac{E_t\left[M_{t,t+s} D_{it+s}\right]}{P_{it}} = 1$.

Expected Returns, Size, and Micro Uncertainty: With constant physical capital over time and across firms, sorting on size and book-to-market leads to the same portfolios, i.e. small market cap firms are the same as high book-to-market ones. In this partial equilibrium framework, the idiosyncratic variation in size is driven by Z_{it}^s. Assuming that the multiplicative dividend payout follows an AR(1) process, the relation between P_{it} and Z_{it} becomes a direct mapping, i.e. $Z_{it}^s = e^{\rho^s z_{it} + \frac{1}{2}\sigma_z^2 \sum_{j=1}^s \rho^{2(j-1)}}$ with $z_{it} = \rho z_{it-1} + \sigma_z \varepsilon_t$. Then, the weights on each dividend strip are:

$$\begin{aligned} \Omega_{it}^s &= \frac{Z_{it}^s P_t^s}{\sum_s Z_{it}^s P_t^s}, \\ &= \frac{e^{\rho^s z_{it} + \frac{1}{2}\sigma_z^2 \sum_{j=1}^s \rho^{2(j-1)}} P_t^s}{\sum_s e^{\rho^s z_{it} + \frac{1}{2}\sigma_z^2 \sum_{j=1}^s \rho^{2(j-1)}} P_t^s}, \\ \frac{\partial \Omega_{it}^s}{\partial z_{it}} &= \left[\rho^s - \left(\sum_\nu \rho^\nu \Omega_{it}^\nu\right)\right]\Omega_{it}^s. \end{aligned}$$

The derivative is positive for small s $\left(\rho - \left(\sum_\nu \rho^\nu \Omega_{it}^\nu\right) > 0\right)$ and negative for large s $\left(-\left(\sum_\nu \rho^\nu \Omega_{it}^\nu\right) < 0\right)$ as an increase in z_{it} tilts the dividend strip weights towards shorter maturities. Thus, large firms (high z_{it}) have a weight structure $\Omega_{it}^s > \Omega_{it}^{s+1}$ while small firms (small z_{it}) exhibit the opposite pattern. As z_{it} directly drives the portfolio weights Ω_{it}, an increase in the dispersion of z between two firms translates into a larger dispersion in portfolio weights, and thus, a larger dispersion in betas. As z follows an AR(1) process the dispersion between firms depends on the level of the conditional uncertainty σ_z and an increase in σ_z increases the dispersion in betas between firms.

Appendix C. Numerics

The policy functions of the model in Section 3 are obtained numerically. First, we discretize the state-space variables x_t, ν_t, $Z_{i,t}$, and $K_{i,t}$. We employ a value function iteration procedure to derive the firm's market value of equity. To maximize the objective function we implement the Nelder-Mead method to find K_{t+1} which maximizes V_t, given $f(K_{t+1}) + E_t[g(K_{t+1})]$. The method uses a simplex to search the domain. Initially, the procedure starts with a randomly generated simplex. For each subsequent iteration, the algorithm reshapes the simplex one vertex at a time towards the optimal region in the search space either via reflection, expansion, contraction, or a shrink contraction. We verify our solution with a simple grid-search algorithm. To approximate the integrals, we apply Gauss-Hermite quadrature and verify the algorithm's accuracy by increasing the number of integration points until the Euler equation errors converge towards zero.

Equilibrium Conditions. To solve for the competitive equilibrium along the balanced growth path, we define the stationary variables $\hat{U}_t \equiv U_t/C_t$, $\hat{K}_{i,t} \equiv K_{i,t}/Z_{t-1}$, $\hat{V}_{i,t} \equiv V_{i,t}/Z_{t-1}$, $\hat{Y}_{i,t} \equiv Y_{i,t}/Z_{t-1}$, $\hat{I}_{i,t} \equiv I_{i,t}/Z_{t-1}$, $\hat{D}_{i,t} \equiv D_{i,t}/Z_{t-1}$, and $\hat{H}_{i,t} \equiv H_{i,t}/Z_{t-1}$ such that the equilibrium conditions read:

- Utility

$$\hat{U}_t = \left((1-\beta) + \beta E_t\left[\left(\hat{U}_{t+1}\frac{C_{t+1}}{C_t}\right)^{1-\gamma}\right]^{\frac{1-1/\psi}{1-\gamma}}\right)^{\frac{1}{1-1/\psi}} \tag{C.1}$$

- Stochastic discount factor

$$M_{t+1} = \beta\left(\frac{C_{t+1}}{C_t}\right)^{-\frac{1}{\psi}} \left(\frac{\left(\hat{U}_{t+1}\frac{C_{t+1}}{C_t}\right)^{1-\gamma}}{E_t\left[\left(\hat{U}_{t+1}\frac{C_{t+1}}{C_t}\right)^{1-\gamma}\right]}\right)^{\frac{1/\psi-\gamma}{1-\gamma}} \tag{C.2}$$

- Output

$$\hat{Y}_{it} = e^{(1-\alpha)(\mu+\phi x_t + z_{it})}\hat{K}_{it}^{\alpha} - f\hat{K}_{it} - \bar{f} \tag{C.3}$$

- Capital accumulation

$$\hat{K}_{it+1}e^{\mu+\phi x_t} = \hat{I}_{it} + (1-\delta)\hat{K}_{it} \tag{C.4}$$

- Adjustment costs

$$\hat{H}_{it} = a_t\hat{K}_{i,t} + \frac{\theta_t}{2}\left(\frac{\hat{I}_{i,t}}{\hat{K}_{i,t}}\right)^2 \hat{K}_{i,t} \tag{C.5}$$

- Firm value

$$\hat{V}_{it} = \max\left(\hat{D}_{it} + e^{\mu+\phi x_t}E_t\left[M_{t,t+1}\hat{V}_{it+1}\right], s\hat{K}_{it}\right) \tag{C.6}$$

$$\hat{D}_{it} = \hat{Y}_{it} - \hat{H}_{it} - \hat{I}_{it} \tag{C.7}$$

- Stock returns

$$R_{it+1} = \frac{\hat{V}_{it+1}}{\hat{V}_{it} - \hat{D}_{it}}e^{\mu+\phi x_t} \tag{C.8}$$

- Exogenous shocks

$$\Delta c_{t+1} = \mu + x_t + \sigma_t \varepsilon_{ct+1} \tag{C.9}$$

$$x_{t+1} = \rho_x x_t + \sigma_x \sigma_t \varepsilon_{xt+1} \tag{C.10}$$

$$\sigma_{t+1} = \bar{\sigma} + \varsigma \nu_{t+1} \tag{C.11}$$

$$\nu_{t+1} = \rho_\nu \nu_t + \sigma_\nu \varepsilon_{\nu t+1} \tag{C.12}$$

$$z_{it+1} = \rho_z z_{it} + \sigma_{zt} \varepsilon_{it+1} \tag{C.13}$$

$$\sigma_{zt+1} = \bar{\sigma}_z + \varsigma_z \nu_{t+1} \tag{C.14}$$

References

Ai, H., Kiku, D., 2015. Volatility risks and growth options. Manage Sci 62 (3), 741–763.
Alfaro, I., Bloom, N., Lin, X., 2018. The finance uncertainty multiplier. Technical Report. National Bureau of Economic Research.
Babenko, I., Boguth, O., Tserlukevich, Y., 2016. Idiosyncratic cash flows and systematic risk. J Finance 71 (1), 425–456.
Bai, H., Hou, K., Kung, H., Li, E.X., Zhang, L., 2019. The CAPM strikes back? an equilibrium model with disasters. J financ econ 131 (2), 269–298.
Bansal, R., Dittmar, R.F., Lundblad, C.T., 2005. Consumption, dividends, and the cross section of equity returns. J Finance 60 (4), 1639–1672.
Bansal, R., Yaron, A., 2004. Risks for the long run: a potential resolution of asset pricing puzzles. J Finance 59 (4), 1481–1509.
Belo, F., Lin, X., 2011. The inventory growth spread. Rev Financ Stud 25 (1), 278–313.
Belo, F., Lin, X., Bazdresch, S., 2014. Labor hiring, investment, and stock return predictability in the cross section. Journal of Political Economy 122 (1), 129–177.
Belo, F., Lin, X., Vitorino, M.A., 2014. Brand capital and firm value. Rev Econ Dyn 17 (1), 150–169.
Berk, J.B., Green, R.C., Naik, V., 1999. Optimal investment, growth options, and security returns. J Finance 54 (5), 1553–1607.
Bloom, N., 2009. The impact of uncertainty shocks. Econometrica 77 (3), 623–685.
Bloom, N., Floetotto, M., Jaimovich, N., Saporta-Eksten, I., Terry, S.J., 2018. Really uncertain business cycles. Econometrica 86 (3), 1031–1065.
Carlson, M., Fisher, A., Giammarino, R., 2004. Corporate investment and asset price dynamics: implications for the cross-section of returns. J Finance 59 (6), 2577–2603.
Christiano, L.J., Fitzgerald, T.J., 2003. The band pass filter. Int Econ Rev (Philadelphia) 44 (2), 435–465.
Clara, N., Corhay, A., Kung, H., 2021. Firm product concentration and asset prices. Available at SSRN 3488428.
Clementi, G.L., Palazzo, B., 2019. Investment and the cross-section of equity returns. J Finance 74 (1), 281–321.
Cooper, R.W., Haltiwanger, J.C., 2006. On the nature of capital adjustment costs. Rev Econ Stud 73 (3), 611–633.
Croce, M.M., 2014. Long-run productivity risk: a new hope for production-based asset pricing? J Monet Econ 66, 13–31.
Crouzet, N., Mehrotra, N.R., 2020. Small and large firms over the business cycle. American Economic Review 110 (11), 3549–3601.
Dew-Becker, I., Giglio, S., 2020. Cross-sectional uncertainty and the business cycle: evidence from 40 years of options data. Technical Report. National Bureau of Economic Research.
Donangelo, A., 2016. Labor leverage and the value premium. Available at SSRN 2668359.
Epstein, L.G., Zin, S.E., 1989. Substitution, risk aversion, and the temporal behavior of consumption and asset returns: a theoretical framework. Econometrica 57 (4), 937–969.
Favilukis, J., Lin, X., 2013. Long run productivity risk and aggregate investment. J Monet Econ 60 (6), 737–751.
Favilukis, J., Lin, X., 2015. Wage rigidity: a quantitative solution to several asset pricing puzzles. Rev Financ Stud 29 (1), 148–192.
Feenstra, R.C., Inklaar, R., Timmer, M.P., 2015. The next generation of the penn world table. American economic review 105 (10), 3150–3182.
Gomes, J., Kogan, L., Zhang, L., 2003. Equilibrium cross section of returns. Journal of Political Economy 111 (4), 693–732.
Gomes, J.F., 2001. Financing investment. American Economic Review 91 (5), 1263–1285.
Gomes, J.F., Kogan, L., Yogo, M., 2009. Durability of output and expected stock returns. Journal of Political Economy 117 (5), 941–986.
Gomes, J.F., Schmid, L., 2010. Levered returns. J Finance 65 (2), 467–494.
Gourio, F., Michaux, M., 2012. Financing investment with long-term debt and uncertainty shocks. Unpublished working paper. University of Southern California.
Herskovic, B., Kelly, B., Lustig, H., Van Nieuwerburgh, S., 2016. The common factor in idiosyncratic volatility: quantitative asset pricing implications. J financ econ 119 (2), 249–283.
Herskovic, B., Kelly, B., Lustig, H., Van Nieuwerburgh, S., 2020. Firm volatility in granular networks. Journal of Political Economy 128 (11), 4097–4162.
Hou, K., Xue, C., Zhang, L., 2020. Replicating anomalies. Rev Financ Stud 33 (5), 2019–2133.
Jordà, Ò., 2005. Estimation and inference of impulse responses by local projections. American economic review 95 (1), 161–182.
Kogan, L., Papanikolaou, D., 2014. Growth opportunities, technology shocks, and asset prices. J Finance 69 (2), 675–718.
Kuehn, L., Schreindorfer, D., Ehouarne, C., 2016. Misallocation cycles. 2016 Meeting Papers. Society for Economic Dynamics.
Kuehn, L.-A., Simutin, M., Wang, J.J., 2017. A labor capital asset pricing model. J Finance 72 (5), 2131–2178.
Kung, H., Schmid, L., 2015. Innovation, growth, and asset prices. J Finance 70 (3), 1001–1037.
Lettau, M., Ludvigson, S.C., Wachter, J.A., 2007. The declining equity premium: what role does macroeconomic risk play? Rev Financ Stud 21 (4), 1653–1687.
Liu, L.X., Whited, T.M., Zhang, L., 2009. Investment-based expected stock returns. Journal of Political Economy 117 (6), 1105–1139.
Menzly, L., Santos, T., Veronesi, P., 2004. Understanding predictability. Journal of Political Economy 112 (1), 1–47.
Newey, W.K., West, K.D., 1987. A simple, positive semi-definite, heteroskedasticity and autocorrelation consistent covariance matrix. Econometrica 55 (3), 703–708.
Santos, T., Veronesi, P., 2004. Conditional betas. Technical Report. National Bureau of Economic Research.
Zhang, L., 2005. The value premium. J Finance 60 (1), 67–103.